SCIENCE CHINA
Earth Sciences

SPECIAL TOPIC: Integrative stratigraphy and timescale of China
•REVIEW•

January 2019 Vol.62 No.1: 324–348
https://doi.org/10.1007/s11430-017-9195-4

# Quaternary integrative stratigraphy and timescale of China

Chenglong DENG[1,2,3*], Qingzhen HAO[2,3,4], Zhengtang GUO[2,3,4,5] & Rixiang ZHU[1,2,3]

[1] *State Key Laboratory of Lithospheric Evolution, Institute of Geology and Geophysics, Chinese Academy of Sciences, Beijing 100029, China;*
[2] *Institutions of Earth Science, Chinese Academy of Sciences, Beijing 100029, China;*
[3] *College of Earth and Planetary Sciences, University of Chinese Academy of Sciences, Beijing 100049, China;*
[4] *Key Laboratory of Cenozoic Geology and Environment, Chinese Academy of Sciences, Beijing 100029, China;*
[5] *CAS Center for Excellence in Tibetan Plateau Earth Sciences, Beijing 100101, China*

Received August 16, 2017; revised November 3, 2017; accepted March 21, 2018; published online May 10, 2018

**Abstract** Quaternary strata in China mainly comprise continental deposits in a variety of depositional settings. The continental Quaternary in temperate northern China consists mainly of eolian and fluvio-lacustrine deposits; that in subtropical southern China, mainly of vermiculated red soils, cave/fissure deposits, and fluvio-lacustrine deposits; and that in the alpine Tibetan Plateau, mainly of fluvio-lacustrine and piedmont deposits. The marine Quaternary in China consists of detrital deposits and biogenic reef deposits. The integration of biostratigraphy, magnetostratigraphy, climatostratigraphy and an astronomically calibrated chronology has led to the establishment of high-precision climatochronostratigraphic timescales for the detrital marine Quaternary in the South China Sea and the loess-paleosol sequence in the Chinese Loess Plateau. Extremely high-precision $^{230}$Th dating has provided a high-precision absolute age model for cave stalagmites over the past 640000 years as well as high-resolution oxygen isotope records representing orbital- to suborbital-scale climate changes. By combining magnetic stratigraphy and biostratigraphy, robust chronostratigraphic frameworks for non-eolian continental Quaternary deposits on the scale of Quaternary geomagnetic polarities have been established. The continental Pleistocene Series consists, from oldest to youngest, of the Nihewanian Stage of the Lower Pleistocene, the Zhoukoudianian Stage of the Middle Pleistocene, and the Salawusuan Stage of the Upper Pleistocene. Stages of the continental Holocene Series have not yet been established. This review summarizes recent developments in the Quaternary chronostratigraphy of representative Quaternary strata and associated faunas, and then proposes an integrative chronostratigraphic framework and a stratigraphic correlation scheme for Quaternary continental strata in China. In the near-future, it is hoped to establish not only a Chinese continental Quaternary climatochronostratigraphic chart on the scale of glacial-interglacial cycles but also a Quaternary integrative chronostratigraphic chart including both continental and marine strata in China.

**Keywords** Quaternary, Chronostratigraphy, Magnetic stratigraphy, Biostratigraphy, Climatostratigraphy, China

**Citation:** Deng C L, Hao Q Z, Guo Z T, Zhu R X. 2019. Quaternary integrative stratigraphy and timescale of China. Science China Earth Sciences, 62: 324–348, https://doi.org/10.1007/s11430-017-9195-4

## 1. Introduction

The Quaternary Period spans the last ~2.6 million years ago to the present and it witnessed the final establishment of global patterns of land-sea distribution, topography, the climate system and terrestrial ecosystems. During the Quaternary, Earth's climate was profoundly influenced by bipolarglaciation and characteristic glacial-interglacial cycles. In particular, the Quaternary is a pivotal period in human evolution, during which the genus *Homo* first appeared and eventually modern humans and finally modern civilization.

*Corresponding author (email: cldeng@mail.iggcas.ac.cn)

The Quaternary Period, following the Neogene Period, consists of the Pleistocene and Holocene Epochs. The Pleistocene has four stages, including two (Gelasian and Calabrian) for the Lower Pleistocene, one for the Middle Pleistocene and one for the Upper Pleistocene. The Gelasian and Calabrian Stages are formally defined by Global Boundary Stratotype and Points (GSSPs) (Aguirre and Pasini, 1985; Rio et al., 1998), while the GSSPs for the Middle Pleistocene and Upper Pleistocene remain to be determined. The base of the Holocene Epoch/Series is defined at 1492.45-m depth in the NGRIP Greenland ice core (Walker et al., 2008).

The base of the Quaternary Period/System was previously defined by the GSSP of the Calabrian Stage, which was placed near the top of the Olduvai normal subchron (~1.8 Ma) (Gradstein et al., 2004). In June 2009, the International Union of Geological Sciences (IUGS) ratified a proposal by the International Commission on Stratigraphy (ICS) to lower the base of the Quaternary Period/System and the Pleistocene Epoch/Series to the GSSP of the Gelasian Stage (Gibbard et al., 2010). The base of the Gelasian Stage, which has an astronomically-tuned age of ~2.6 Ma, corresponds to Marine Isotope Stage (MIS) 103 and the Gauss-Matuyama (G-M) geomagnetic reversal (Figure 1). The climatostratigraphy and chronostratigraphy of the loess-paleosol sequence of the Chinese Loess Plateau (CLP) provide strong support for the proposal.

The Quaternary strata in China are mostly of continental origin and consist mainly of eolian, fluvial, lacustrine, cave/fissure and piedmont deposits, which are typically rich in mammalian fossils (Figures 2 and 3, Tables 1 and 2). The Quaternary marine strata in China are developed in the continental shelf seas and marginal seas of eastern and southern China. They comprise continental deposits in the Bohai Sea, Yellow Sea, East China Sea and South China Sea, and carbonate biogenic reefs in the South China Sea.

In early studies, the establishment of chronostratigraphic frameworks for Quaternary continental strata relied mainly on biostratigraphy. The widespread and successful use of magnetostratigraphy to date Chinese Quaternary strata from the 1970s and the resulting breakthroughs in loess climatostratigraphy led Professor Liu Tungsheng and his collea-

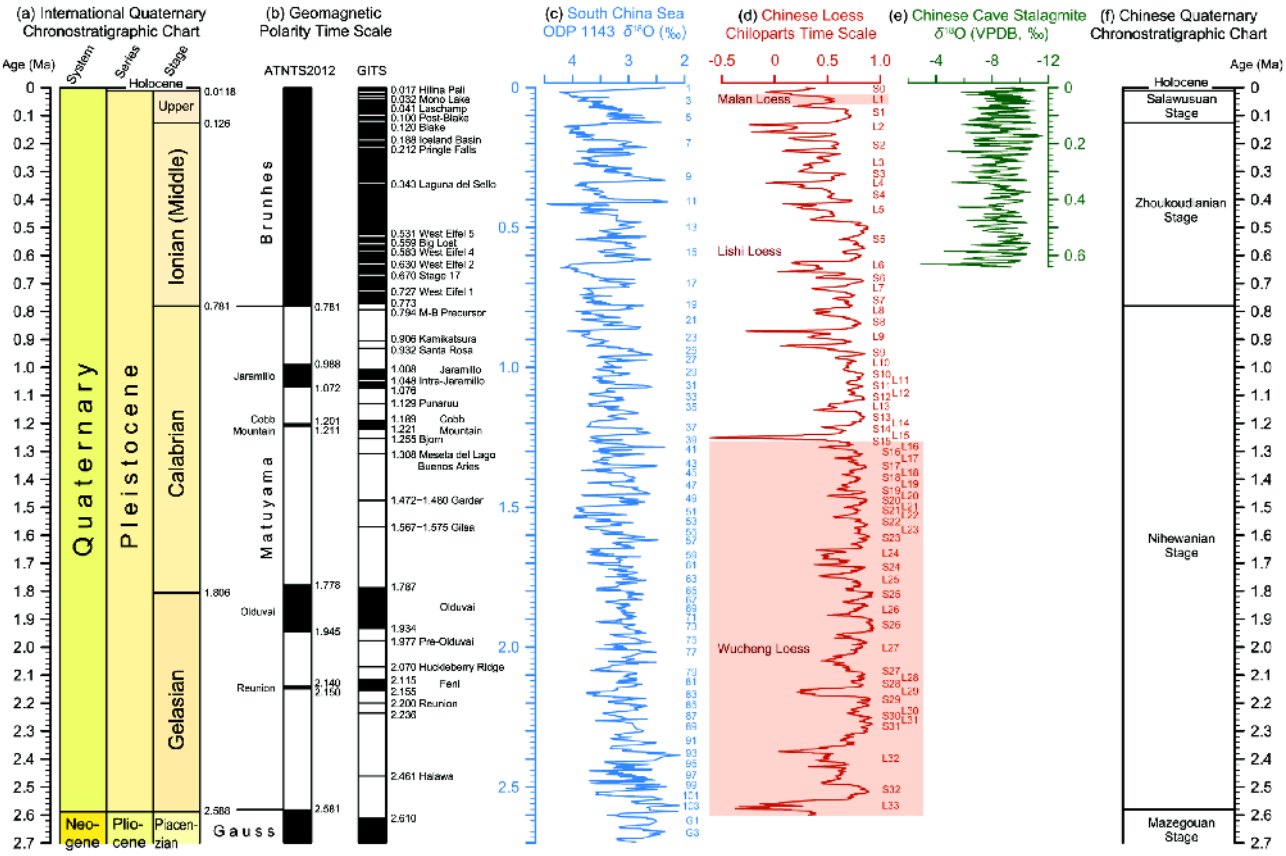


**Figure 1** Chinese Quaternary chronostratigraphy and its correlation with the international Quaternary chronostratigraphic chart and the geomagnetic polarity timescale. (a) The international Quaternary chronostratigraphic chart (Pillans and Gibbard, 2012). (b) The astronomically tuned Neogene timescale of Hilgen et al. (2012) (ATNTS2012) and the Quaternary geomagnetic instability timescale (GITS) (Singer, 2014; Singer et al., 2014). (c) Benthic $\delta^{18}$O records for ODP Site 1143 in the South China Sea (Tian et al., 2002). The numbers indicate marine oxygen isotope stages. (d) Chinese loess Chiloparts timescale (Ding et al., 2002). L and S respectively represent loess and paleosol units. (e) $\delta^{18}$O stack of Chinese cave stalagmites over the past 640000 years (Cheng et al., 2016). (f) The Chinese Quaternary chronostratigraphic chart (National Commission on the Stratigraphy of China, 2017).

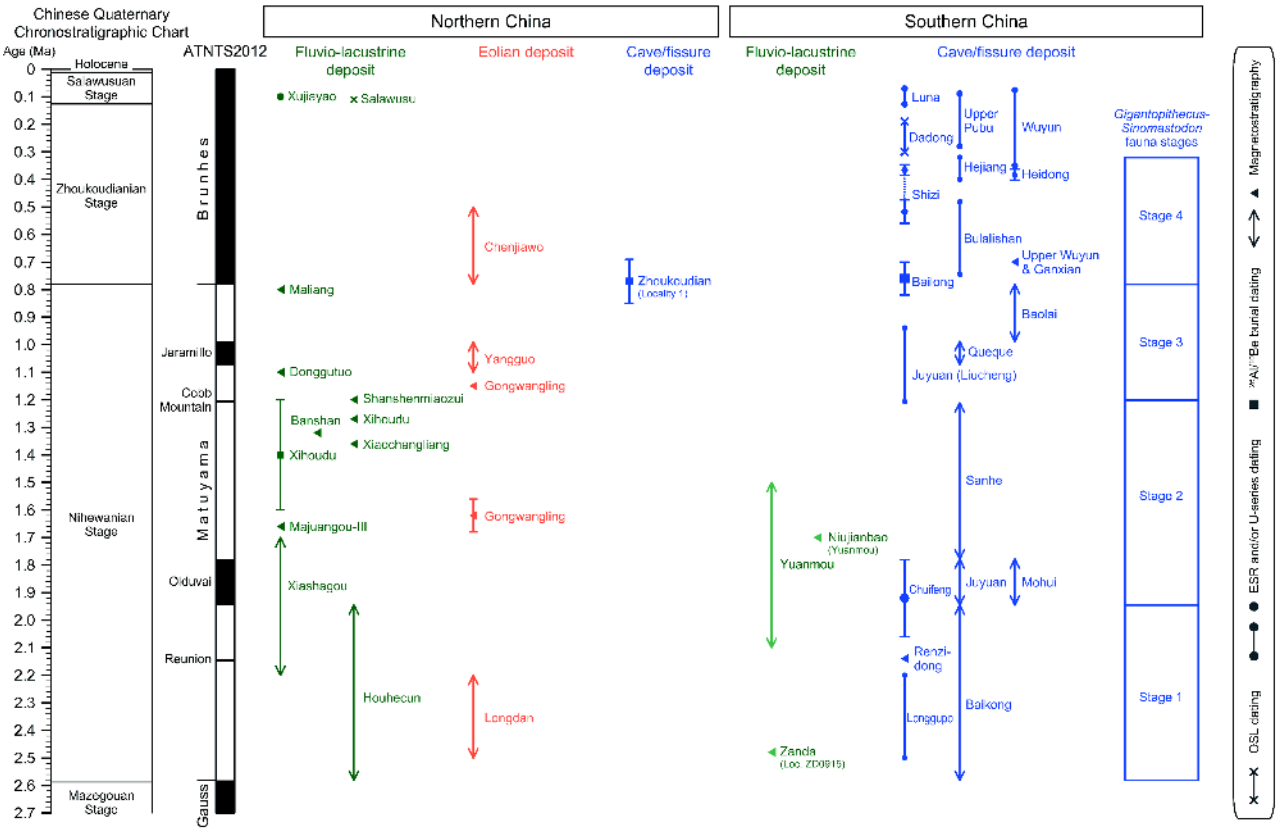


**Figure 2** A synthesis diagram relating the well-dated Quaternary mammalian faunas in China to the Chinese Quaternary chronostratigraphic chart (National Commission on the Stratigraphy of China, 2017) and the ATNTS2012 timescale (Hilgen et al., 2012). See text and Tables 1 and 2 for age data and references.

gues to propose a Chinese Quaternary chronostratigraphic chart based mainly on correlation with marine oxygen isotope records (Liu et al., 2000). Since the 2000s, considerable advances in high-precision isotopic chronology of stalagmites, the oxygen isotope stratigraphy of ODP Leg 184 borehole sequences in the South China Sea, and the magnetostratigraphy of continental sedimentary sequences have contributed to an improved understanding of Chinese Quaternary chronostratigraphy. In the future, it will be possible to establish a Chinese Quaternary climatochronostratigraphic framework constrained by high-precision chronologies provided by multi-disciplinary dating methods, which will enable regional and global stratigraphic correlations as well as stratigraphic correlations between continental and marine realms.

## 2. A brief history of Chinese Quaternary chronostratigraphic studies

Early attempts to date the Quarternary strata in China began during the 1920s−1930s with biostratigraphic investigations in northern China. For example, in 1922 Emile Licent and Pierre Teilhard de Chardin made excavations in the drainage area of the Salawusu River and discovered plentiful mammalian fossils, including teeth of *Homo sapiens*, and Paleolithic artifacts (Teilhard de Chardin and Licent, 1924). Later, in 1930 the publication of *Les mammifères fossiles de Nihowan (Chine)* by Teilhard de Chardin and Piveteau was an important step, and since then the Nihewan Basin has attracted intensive research attention worldwide. In 1933, in *Fossil Man in China*, Davidson Black, Pierre Teilhard de Chardin, Chungchien Young and Wenchung Pei synthesized systematic investigations of the Zhoukoudian site (Peking Man site) as well as the developments in Chinese Quaternary biostratigraphy at that time. In addition, the synthesis of Black et al. (1933) brought Peking Man to global attention. These pioneering biostratigraphic researches paved the way for establishing chronostratigraphic frameworks for the continental Quaternary in China.

Early studies on Quaternary biostratigraphy focused mainly on specific faunas due to the lack of precise and accurate age constraints. The increasing amount of research on the biostratigraphy of Chinese Quaternary strata, and the resulting growing database of terrestrial biochronostratigraphy, enabled the establishment of mammal-based chronological systems (that is, land mammal stages/ages, LMS/As). However, except for Quaternary LMS/As, Paleogene

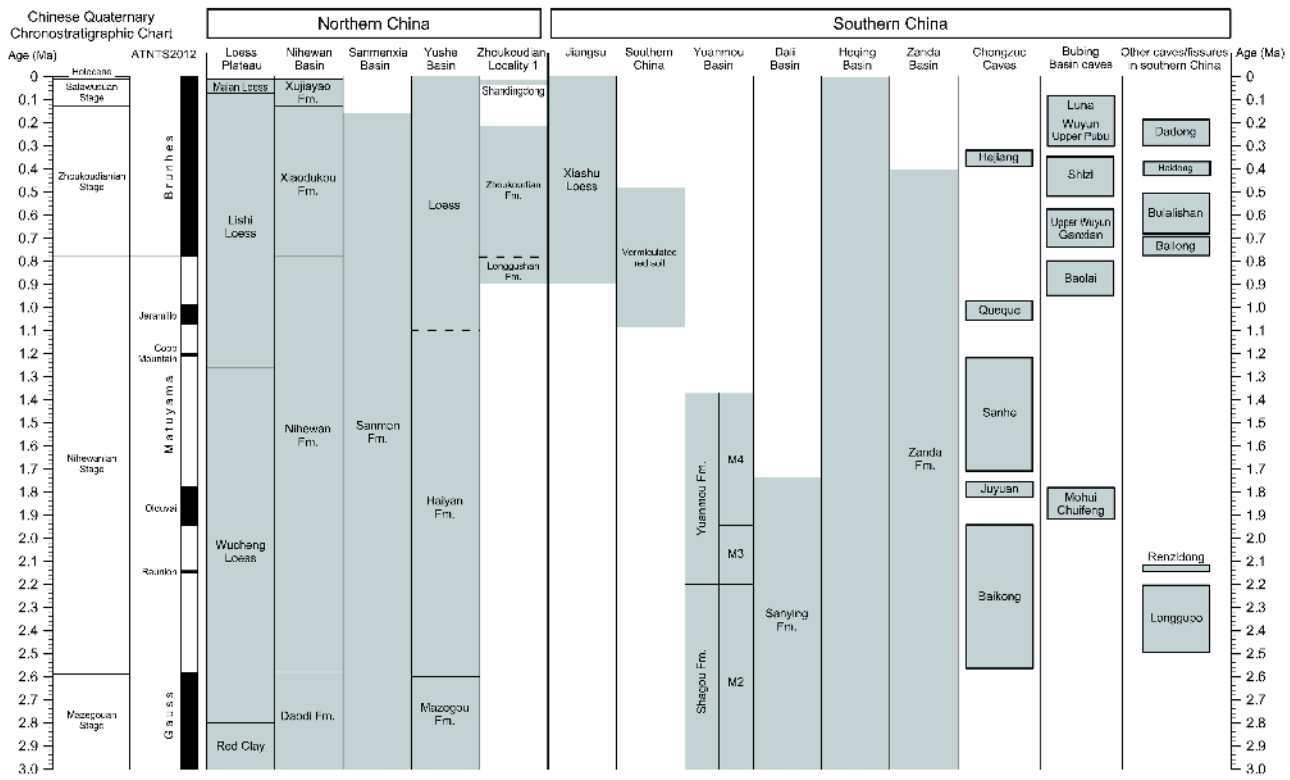


**Figure 3** Correlation and division of the Chinese Quaternary terrestrial strata indicated by the shaded area. See text for age data and references.

**Table 1** Chronology of mammalian fossil sites in continental Quaternary of northern China

| Sedimentary facies | Regions | Sites | Age (Ma) | Dating methods | References |
|---|---|---|---|---|---|
| Fluvio-lacustrine deposits | Nihewan Basin | Xujiayao | 0.1 | U-series | Chen et al., 1982 |
| | | Maliang | 0.8 | Magnetostratigraphy | Wang et al., 2005a |
| | | Donggutuo | 1.1 | Magnetostratigraphy | Wang et al., 2005a |
| | | Shanshenmiaozui | 1.2 | Magnetostratigraphy | Liu et al., 2016b |
| | | Banshan | 1.32 | Magnetostratigraphy | Zhu et al., 2004 |
| | | Xiaochangliang | 1.36 | Magnetostratigraphy | Zhu et al., 2001 |
| | | Majuangou-III | 1.66 | Magnetostratigraphy | Zhu et al., 2004 |
| | | Xiashagou | 2.2−1.7 | Magnetostratigraphy | Liu et al., 2012 |
| | Sanmenxia Basin | Xihoudu | 1.27 | Magnetostratigraphy | Zhu et al., 2003 |
| | | | 1.4±0.2 | $^{26}Al/^{10}Be$ burial | Kong et al., 2013 |
| | Hetao Basin | Salawusu | 0.15−0.075 | TL, OSL, $^{14}C$ | Min et al., 2009 |
| Eolian deposits | Weihe Basin (Sanmenxia Basin) | Gongwangling | 1.15 | Magnetostratigraphy | An and Ho, 1989 |
| | | | 1.62 | Magnetostratigraphy | Zhu et al., 2015b |
| | | Chenjiawo | 0.78−0.50 | Magnetostratigraphy | Yue and Xue, 1996 |
| | | Yangguo | 1.10−0.99 | Magnetostratigraphy | Yue et al., 1994 |
| | Linxia Basin | Longdan | 2.5−2.2 | Magnetostratigraphy | Zan et al., 2016 |
| Cave/fissure deposits | North China Plain | Locality 1, Zhoukoudian | 0.77±0.08 | $^{26}Al/^{10}Be$ burial | Shen et al., 2009 |

and Neogene LMS/As today constitute an important part of the Cenozoic Geologic Time Scale (Gradstein et al., 2012).

The efforts to establish Chinese LMS/As for the Quaternary can be traced at least to Pei's (1957) pioneering work, in which he proposed four and two Quaternary mammalian faunas with different ages in northern and southern China, respectively, based on zoogeographical divisions of mammalian faunas. Later, increasing efforts were made to es-

**Table 2** Chronology of mammalian fossil sites in continental Quaternary of southern China

| Sedimentary facies | Regions | Sites | Age (Ma) | Dating methods | References |
|---|---|---|---|---|---|
| Fluvio-lacustrine deposits | Yuanmou Basin | Niujianbao | 1.7 | Magnetostratigraphy | Zhu et al., 2008b |
| | | Yuanmou Basin | 2.1−1.5 | Magnetostratigraphy | Zhu et al., 2008a, 2008b; Qian and Zhou, 1991 |
| | Zanda Basin | IVPP ZD0915 | 2.48 | Magnetostratigraphy | Wang et al., 2013b |
| Cave/fissure deposits | Chongzuo, Guangxi | Baikong Cave | 2.58−1.95 | Magnetostratigraphy | Sun et al., 2014 |
| | | Juyuan Cave | 1.95−1.78 | Magnetostratigraphy | Sun et al., 2014 |
| | | Sanhe Cave | 1.78−1.07 | Magnetostratigraphy | Sun et al., 2014 |
| | | Queque Cave | 1.07−0.99 | Magnetostratigraphy | Sun et al., 2014 |
| | | Hejiang Cave | 0.4−0.32 | U-series | Zhang et al., 2014 |
| | Bubing Basin | Chuifeng Cave | 1.92±0.14 | ESR, U-series, magnetostratigraphy | Shao et al., 2014 |
| | | Mohui Cave | 1.95−1.78 | Magnetostratigraphy | Sun et al., 2017a |
| | | Baolai Cave | 0.99−0.78 | Magnetostratigraphy | Sun et al., 2017a |
| | | Upper Wuyun Cave | 0.7 | Magnetostratigraphy | Sun et al., 2017a |
| | | Ganxian Cave | 0.7 | Magnetostratigraphy | Sun et al., 2017a |
| | | Shizi Cave | 0.517−0.366 | U-series | Kong et al., 2012 |
| | | Wuyun Cave | 0.35−0.20 | U-series | Wang et al., 2007a |
| | | | 0.279−0.076 | ESR | Rink et al., 2008 |
| | | Upper Pubu Cave | 0.28−0.088 | ESR | Rink et al., 2008 |
| | | Luna Cave | 0.127−0.07 | U-series | Bae et al., 2014 |
| | Wushan, Chongqing | Longgupo | 2.5−2.2 | ESR, U-series | Han et al., 2017 |
| | Liucheng, Guangxi | Juyuan Cave (*Gigantopithecus* Cave) | 1.206−0.94 | ESR, U-series | Rink et al., 2008 |
| | Wuming, Guangxi | Bulali Hill | 0.745−0.481 | ESR | Rink et al., 2008 Jin et al., 2009 |
| | Daxin, Guangxi | Black Cave (Heidong Cave) | 0.383±0.02 | ESR, U-series | Shao et al., 2017 |
| | Yunxian, Hubei | Bailong Cave | 0.76±0.06 | $^{26}Al/^{10}Be$ burial | Liu et al., 2015 |
| | Panxian, Guizhou | Dadong Cave | 0.3−0.19 | OSL | Zhang et al., 2015 |
| | Fanchang, Anhui | Renzidong | 2.15−2.14 | Magnetostratigraphy | Wang et al., 2012 |

tablish Chinese LMS/As for the Quaternary, which, however, mainly concerned the Nihewanian Stage/Age of the Early Pleistocene (Qiu and Qiu, 1995; Qiu, 2000; Deng, 2006; Wang et al., 2013a).

Since the third National Conference on Stratigraphy in 2000, considerable progress has been made toward establishing Chinese LMS/As for the Quaternary. The continental Pleistocene Series in China has three stages, including, from oldest to youngest, the Lower Pleistocene Nihewanian Stage, the Middle Pleistocene Zhoukoudianian Stage, and the Upper Pleistocene Salawusuan Stage, which have been incorporated in the Chinese Chronostratigraphic Chart (2014) (National Commission on the Stratigraphy of China, 2017).

Since climate changes have strongly affected sediment production and sedimentary processes during the Quaternary, including weathering, erosion, transportation and deposition, climatostratigraphy affords a key basis for stratigraphic division and correlation of the continental Quaternary. An outstanding example involves the chronostratigraphy of the CLP loess-paleosol sequence, which highlights the research of Chinese continental Quaternary chronostratigraphy. Based on characteristic assemblages of mammalian fossils, Liu and Zhang (1962) proposed that the Chinese loess strata comprise, from top to bottom, the Malan Loess, Lishi Loess and Wucheng Loess, which are respectively of Late Pleistocene, Middle Pleistocene and Early Pleistocene ages. Subsequently, Heller and Liu (1982, 1984, 1986) constructed accurate age models for the CLP loess-paleosol sequence using magnetostratigraphic and climatostratigraphic methods. This breakthrough in chronostratigraphy made Chinese loess an indispensable part of global climate change research. Later developments in the orbital tuning of paleoclimatic proxy records resulted in astronomical timescales that significantly improved the accuracy and

precision of age models for the CLP loess-paleosol sequence (Ding et al., 1994, 2002; Lu et al., 1999; Heslop et al., 2000; Sun et al., 2006). Specifically, these advances in the chronostratigraphy of the CLP loess-paleosol sequence provide strong support for placing the base of the Quaternary Period/System and the Pleistocene Epoch/Series at the Gelasian GSSP, which has an age ~2.6 Ma, rather than at the Calabrian GSSP, which has an age ~1.8 Ma (Gibbard et al., 2010; Yao and Liu, 2010).

In addition to the CLP loess-paleosol sequence, other Quaternary continental strata in China, including fluvio-lacustrine and cave/fissure sedimentary sequences, have been well dated using magnetic stratigraphy. Establishing temporal control for the strata bearing Yuanmou Man and Peking Man by way of magnetic stratigraphy were key developments in early studies (Li et al., 1976; Liu et al., 1977). With the improved understanding of paleomagnetic remanence acquisition processes and the increasing use of SQUID magnetometers since the 1980s, the chronologies of a variety of sedimentary strata and associated faunas have been well constrained (Figures 2 and 3, Tables 1 and 2). The purpose of the present contribution is to review recent developments provided mainly by magnetostratigraphic investigations of continental Quaternary strata and associated faunas, and then to propose an integrative chronostratigraphic framework and a stratigraphic correlation scheme for Quaternary continental strata in China (Figures 1–3). In addition, we propose several critical issues in Chinese Quaternary chronostratigraphy which are currently unresolved. However, certain sedimentary units lacking robust age constraints (e.g. the Xigeda Formation in southwestern China and the Xiyu Formation in northwestern China) are not discussed here.

## 3. Subdivision of the continental Quaternary in China

In the Chinese Quaternary Chronostratigraphic Chart (2014), the Pleistocene Series consists, from oldest to youngest, of the Nihewanian Stage of the Lower Pleistocene, the Zhoukoudianian Stage of the Middle Pleistocene, and the Salawusuan Stage of the Upper Pleistocene. Stages of the Holocene Series have not yet been established.

### 3.1 Nihewanian Stage

The Nihewanian Stage represents the Lower Pleistocene of the Chinese Quaternary. In 1999 the Quaternary Working Group of the National Commission on the Stratigraphy of China proposed the Nihewanian Stage, which was named from the lithostratigraphic unit of the Nihewan Formation. The Xiashagou section in the eastern margin of the Nihewan Basin could serve as one of the candidates for the stratotype section of the Nihewanian Stage, because the section not only yields an almost complete fluvio-lacustrine sequence of the Nihewan beds and associated classic Xiashagou fauna (Teilhard de Chardin and Piveteau, 1930), but also records the G-M geomagnetic reversal (Liu et al., 2012), which provides a key correlation event for the basal boundary of the Quaternary System and the Pleistocene Series (Gibbard et al., 2010). In addition, Li et al. (1984) proposed the Nihewanian Age as the land mammal age of the early Quaternary, which is named from the Nihewan fauna (*sensu stricto*), that is, the Xiashagou fauna. Thus, the Nihewanian Stage as a chronostratigraphic unit and the Nihewanian Age as a land mammal age are well consistent.

The Nihewan beds are rich in mammalian fossils, known as the Nihewan faunas (*sensu lato*). In particular, the Nihewan fauna (*sensu stricto*) only represents the Xiashagou fauna, which was first reported by Teilhard de Chardin and Piveteau (1930). This fauna consists of mammalian fossils collected from the Xiashagou section and its adjacent sections near Xiashagou village. Later, the faunal list of the Xiashagou fauna was revised by Zhou et al. (1991) and Qiu and Qiu (1995). The age of the Xiashagou section and the associated Xiashagou fauna is of great significance for improving Chinese Quaternary mammal biochronology.

Qiu (2000) conducted a systematic comparison between the Xiashagou faunal elements and those of Villafranchian age in Europe based on 20 commonly shared mammals at generic and/or specific level. The comparison led Qiu (2000) to conclude that the Xiashagou fauna is chronologically close to the Olivola fauna in the early Late Villafranchian age and further to estimate its age as ~1.8 Ma.

The exact stratigraphic positions of the faunal elements of the Xiashagou fauna are unknown. Nevertheless, three sedimentary layers in the Xiashagou section, which span most of the sedimentary interval bearing the Xiashagou fauna, were determined by Professor Wei Qi to have been excavated by local villagers. Recently, high-resolution magnetostratigraphic investigations (Liu et al., 2012) showed that the Xiashagou sedimentary sequence recorded the Brunhes normal chron, the Matuyama reversed chron and the late Gauss normal chron. The Xiashagou fauna resides in the Matuyama reversed chron (between the pre-Reunion Matuyama chron and the post-Olduvai Matuyama chron), yielding an estimated age of ~2.2–1.7 Ma. The Pliocene-Pleistocene boundary (G-M boundary) is in the lower part of the Xiashagou section. Therefore, a chronological consensus for the Xiashagou fauna has been reached independently, on both magnetostratigraphic and biostratigraphic grounds.

The Nihewanian Stage corresponds to the combination of the Gelasian and Calabrian Stages, and its basal boundary is consistent with that of the Gelasian Stage, corresponding to the G-M boundary. Thus, the basal age of the Nihewanian Stage is the same as that of the Gelasian Stage, which has

been determined to be 2.588 Ma in the Geologic Time Scale 2012 (Pillans and Gibbard, 2012). The lower boundary of the Nihewanian Stage as well as the G-M boundary are well recorded in the lowest part of the Xiashagou section (Liu et al., 2012). Sediments near the boundary consist of fluvio-lacustrine silts, sandy silts and fine-grained sands. However, more silts and silty clays with a red color and of fluvio-lacustrine origin were found to occur in the sediments beneath the boundary, which are derived from the reworked and redeposited eolian red clay formation (Deng et al., 2008).

The Nihewanian Stage is characteristic of the *Proboscidipparion-Equus* fauna. However, a chronospecies marking its basal boundary has not yet been determined. Deng and Xue (1997) have suggested that the first appearance of the genus *Equus* in Eurasia can be regarded as indicating the lower boundary of the Quaternary as well as that of the Nihewanian Stage. In recent years, magnetostratigraphic dating of mammalian faunas in a series of sedimentary basins has provided support for this viewpoint. For example, *Equus* fossils occur in many sites in the eastern Nihewan Basin of northern China, such as Maliang, Donggutuo, Banshan, Xiaochangliang, Shanshenmiaozui, Majuangou, Xiashagou and Danangou. Among those sites, the Maliang site, paleomagnetically dated to ~0.8 Ma (Wang et al., 2005a), is the youngest; and the Xiashagou or Danangou sites, paleomagnetically and/or biostratigraphically estimated to 2.0−1.8 Ma, are the oldest (Qiu, 2000; Deng et al., 2008; Liu et al., 2012).

In the Yuanmou Basin in the southeastern margin of the Tibetan Plateau, *Equus yunnanensis* fossils occur in the stratigraphic interval from Bed 18 of middle M3 to Bed 27 of upper M4 of the Yuanmou Formation (Qian and Zhou, 1991), and have been paleomagnetically dated to 2.1−1.5 Ma (Zhu et al., 2008a, 2008bb). In the Linxia Basin in the northeastern margin of the Tibetan Plateau, the *Equus*-bearing Longdan fauna was recently paleomagnetically dated to 2.5−2.2 Ma (Zan et al., 2016). In the Zanda Basin in the southwestern margin of the Tibetan Plateau, the local first appearance of *Equus* (IVPP locality ZD0915) was paleomagnetically dated to 2.48 Ma (Wang et al., 2013b).

In addition, our unpublished paleomagnetic results obtained from sedimentary basins in north-central China show that the *Equus* fossils in the Haiyan Formation of the Yushe Basin occur just above the upper boundary of the Olduvai normal subchron and have an age of ~1.7 Ma; and that the *Equus*-bearing Houhecun fauna in the Weihe Basin (Wang, 1988) occurs in the early Matuyama reversed chron, close to the G-M boundary, that is, the beginning of the Quaternary.

These various lines of evidence for the age constraints of fossil *Equus* over mainland East Asia indicate a rapid spread of the monodactylid horse as soon as it arrived in the Old World, further highlighting its usefulness as a chronospecies (Wang et al., 2013b).

### 3.2 Zhoukoudianian Stage

The Zhoukoudianian Stage, which was named after the Zhoukoudian locality, Fangshan District of Beijing by Pei et al. (1963), represents the Middle Pleistocene of the Chinese Quaternary. The stratotype section is in the Ordovician limestone caves at Locality 1 of Zhoukoudian. The name of this stage is derived from the lithostratigraphic unit of the Zhoukoudian Formation. The cave deposits of the Zhoukoudian Formation, which yielded the famous fossils of Peking Man, are divided into 13 layers with a total thickness of ~40 m (Wu et al., 1985). The sedimentary sequence is mainly composed of limestone breccia, breccia-bearing clays, silts, sands and gravels interbedded with ash layers, calcareous cemented layers and gravel beds influenced by fluviation. The strata underlying the Zhoukoudian Formation (layers 1 to 13) consist of sedimentary layers 14 to 17 while layers 14 and 15 constitute the Longgushan Formation (Figure 3).

The abundant vertebrate fossils excavated from the Zhoukoudian Formation are designated the Zhoukoudian fauna, which is an important member of the Middle Pleistocene faunas in northern China. 62 taxa of fossil birds (Hou, 1985) and 97 taxa of fossil mammals (Hu, 1985) were identified from Locality 1 of Zhoukoudian. The Zhoukoudian fauna contains typical index fossils *Homo erectus pekinensis* and *Megaloceros pachyosteus* of the Middle Pleistocene. There are also several other species with specific biochronological significance, including *Macaca robustus*, *Trogontherium cuvieri*, *Ochotona koslowi*, *Cricetulus varians*, *Hyaena sinensis*, *Equus sanmeniensis*, *Ursus spelaeus*, *Machairodus inexpectatus*, *Palaeoloxodon* cf. *namadicus*, *Dicerorhinus choukoutienensis*, *Paracamelus gigas*, *Bubalus teilhardi*, *Spirocerus peii*, *Hystrix subcristata*, and *Felis youngi*.

The age constraints on Locality 1 of Zhoukoudian derive from a variety of dating methods, such as paleomagnetism, fission track, thermoluminescence (TL), uranium series, electron spin resonance (ESR) and cosmogenic $^{26}Al/^{10}Be$ burial. The results show that the Zhoukoudian Formation began to be deposited since ~780 ka and ceased at ~200 ka (Chen and Zhou, 2009). The Matuyama-Brunhes (M-B) geomagnetic reversal occurs between layers 13 and 14 (Qian et al., 1985). In particular, Shen et al. (2009) obtained a cosmogenic $^{26}Al/^{10}Be$ burial age of 0.77±0.08 Ma from lower cultural layers 7−10. This cosmogenic $^{26}Al/^{10}Be$ burial age may be slightly older if the location of the M-B boundary revealed by paleomagnetism is taken into consideration. Nevertheless, Shen et al.'s (2009) finding provides an independent age constraint for the strata and associated fauna in Zhoukoudian.

In the Chinese Chronostratigraphic Chart (2014), the Zhoukoudianian Stage is correlated with the Ionian Stage

(Middle Pleistocene Subseries). The base of the Zhoukoudianian Stage coincides with that of the Ionian Stage, which is consistent with the M-B boundary and has an age of 781 ka in the astronomically tuned Neogene time scale of Hilgen et al. (2012) (ATNTS2012). Thus, the Zhoukoudian Formation can be confidently assigned to the Middle Pleistocene based on currently available age data. Although the M-B boundary was recognized between layers 13 and 14 in the deposits of Locality 1 (Qian et al., 1985), its precise location remains undetermined due to the limitations resulting from the specific conditions of previous studies (e.g., low sampling resolution, use of an astatic magnetometer for remanence measurements, and the lack of rock magnetic constraints). To precisely determine the location of the M-B boundary (that is, the base of the Zhoukoudianian Stage) in this locality, high-resolution magnetostratigraphy strengthened by high-precision radiometric dating and detailed biostratigraphy is required, and the associated paleomagnetic remanence measurements should be made using a SQUID cryogenic magnetometer installed in a magnetically-shielded space.

### 3.3 Salawusuan Stage

The Salawusuan Stage represents the Upper Pleistocene of the Chinese Quaternary. In 1999 the Quaternary Working Group of the National Commission on the Stratigraphy of China proposed the Salawusuan Stage, which was named from the lithostratigraphic unit of the Salawusu Formation in the drainage area of the Salawusu River in Inner Mongolia, northern China. The stratotype section is in the Jiufangtai section at Wuding River Town of Wushen Banner, Inner Mongolia (Min et al., 2009).

The Jiufangtai section, described in detail by Min et al. (2009), consists of three lithologic formations. The Lishi Loess of the Middle Pleistocene lies at the bottom of the section. The Salawusu Formation of the early Late Pleistocene occupies the middle part of the section, which is composed of clays and clayey silts of limnetic facies intercalated with fluvial fine-grained sands. The Salawusu Formation can be further divided into five lithologic members, including, from oldest to youngest, Member 1 to Member 5. The Chengchuan Formation of the late Late Pleistocene, consisting mainly of fluvial fine-grained sands, constitutes the uppermost part of the section. The Chengchuan Formation can be further divided into three lithologic members, including, from oldest to youngest, Member 1 to Member 3. The base of the Salawusuan Stage lies at the bottom of Member 3 of the Salawusu Formation.

The Salawusu Formation yields abundant vertebrate fossils, including Hetao Man, known as the Salawusu fauna. The faunal assemblage comprises 33 taxa of Mammalia and 12 taxa of Aves (Tong et al., 2008). There are many common members of the Late Pleistocene in northern China in the Salawusu fauna, including *Canis lupus*, *Crocuta ultima*, *Equus* cf. *przewalskii*, *Equus hemionus*, and *Bos primigenius*. Some of the members emerged during the Middle Pleistocene (e.g., *Palaeoloxodon naumanni* and *Cervus elaphus*). In addition, *Megaloceros ordosianus* and *Bubalus wansjocki* were found at Salawusu for the first time (Tong et al., 2008).

Chronological studies of the Salawusu and Chengchuan Formations in different sections (e.g., Jiufangtai, Milanggouwan, Dishaogouwan) in the Salawusu area were carried out using various methods (e.g., TL, optically stimulated luminescence (OSL) and radiocarbon dating). The results show that the Salawusuan Stage began at ~150 ka and ended at ~10 ka. The boundary between the upper and lower Salawusuan Stage, represented by the boundary between the Chengchuan Formation and its underlying Salawusu Formation, can be dated to ~75 ka (Min et al., 2009). Thus, the Salawusu Formation (lower part of the Salawusuan Stage) can be correlated with the last interglacial soil S1 of the Chinese Loess Plateau and MIS 5, while the Chengchuan Formation (upper part of the Salawusuan Stage) corresponds to the Malan Loess (L1) and MIS 2−4 (Li et al., 2004a). In the Chinese Chronostratigraphic Chart (2014), the Salawusuan Stage is correlated with Upper Pleistocene Subseries (Tarantian Stage) of the Geologic Time Scale 2012 (Gradstein et al., 2012). The base of the Salawusuan Stage coincides with that of the Upper Pleistocene Subseries, which has an age of 126 ka. Nevertheless, more precise chronological data are needed to constrain the exact location of the base of the Salawusuan Stage in typical sections.

## 4. Chronostratigraphy of representative Quaternary sedimentary sequences in China

### 4.1 Eolian deposits

#### *4.1.1 Loess-paleosol sequence of the Chinese Loess Plateau (CLP)*

The late Cenozoic eolian deposits in northern China consist of the CLP loess-paleosol sequence of Late Pliocene to Quaternary time (Liu, 1985; Ding et al., 2002; Yang and Ding, 2010), the red clay formation of Late Miocene to Pliocene time in the eastern CLP (Sun et al., 1997; Ding et al., 1998), and the eolian deposits of Miocene to Pliocene time in the western CLP (Guo et al., 2002; Hao and Guo, 2004; Ge et al., 2012; Guo, 2017). In particular, the CLP loess-paleosol sequence of Late Pliocene to Quaternary time, covering an area of more than 400000 $km^2$ in north-central China (Liu, 1985), is extensively distributed from the Qilian Mountains in the west to the Taihang Mountains in the east, and from the southern margin of the Tengger Desert in the north to the northern Qinling Mountains in the south.

The CLP loess-paleosol sequence of Late Pliocene to

Quaternary time consists, from top to bottom, of Holocene loess (L0) and black loam (S0), Pleistocene loess/paleosol units (L1/S1 to L33), and Late Pliocene loess/paleosol units (S33 and L34) (Liu, 1985; Ding et al., 2002; Yang and Ding, 2010). The last glacial loess unit L1 was previously named the Malan Formation; the loess/paleosol couplets from S1/L2 to S14/L15, the Lishi Formation; and the loess/paleosol couplets from S15/L16 to S32/L33, the Wucheng Formation (Liu, 1985; Ding and Liu, 1989).

Since the 1970s, the CLP loess-paleosol sequence has attracted the attention of scientists in the areas of paleoclimatic, paleoenvironmental and geochronological research because of its great significance for the study of past global changes and the associated need for high-precision timescales. Considerable progress has been made during the past four decades in dating the sequence, yielding more and more accurate and precise timescales. Developments in the chronostratigraphy of the CLP loess-paleosol sequence can be divided into three categories, which are discussed in detail below.

The first category concerns magnetic stratigraphy. Initially, the chronology of the CLP loess-paleosol sequence was established mainly through magnetostratigraphic investigations. The pioneering work of Heller and Liu (1982) showed that the loess-paleosol sequence extends back to the early Matuyama reversed chron based on magnetostratigraphic investigations of the Luochuan borehole sequence, thus providing a basal age estimate of the loess-paleosol sequence of ~2.4 Ma, although the G-M geomagnetic reversal was not found in the Luochuan borehole sequence. As a landmark study, Heller and Liu (1982) laid the foundation for the first-order chronostratigraphic framework for the CLP loess-paleosol sequence, which has been subsequently improved and strengthened by further magnetostratigraphic data from numerous loess sections.

Traditionally, the base of the CLP loess-paleosol sequence was designated at the bottom of loess unit L33 (Ding et al. (2002). Recently, based on investigations of magnetic susceptibility, grain size and the magnetostratigraphy of four sections (Lingtai, Jingchuan, Baoji and Lantian) in the central-southern CLP, Yang and Ding (2010) identified a typical loess layer within the uppermost red clay formation, and designated it L34. In addition, they further designated the paleosol unit between loess units L33 and L34 as paleosol unit S33, thus lowering the basal age of the CLP loess-paleosol sequence from 2.6 Ma to 2.8 Ma, convincingly indicating that the CLP loess-paleosol sequence is of Late Pliocene to Holocene age.

There is currently a consensus that the CLP loess-paleosol sequence records the upper Gauss chron, Matuyama chron, and Brunhes chron, as well as the Olduvai and Jaramillo subchrons within the Matuyama chron. The G-M and M-B boundaries and the upper and lower boundaries of the Olduvai and Jaramillo subchrons provide stringent age controls on the chronostratigraphic framework of the CLP loess-paleosol sequence.

The G-M boundary occurs within loess unit L33 (Yang and Ding, 2010). However, the locations of the M-B boundary are variable, as summarized by Qiang et al. (2016). For example, in the northwestern CLP the M-B boundary was found to be in the middle-lower part of paleosol S7 or in the upper part of loess unit L8. However, in the southeastern CLP the boundary was found to be in the lower part of L8 or in the transition zone between L8 and S8.

The differences in the locations of the M-B boundary may be the result of a displaced ('delayed') acquisition of remanent magnetization (Zhou and Shackleton, 1999; Wang et al., 2006). However, there are no apparent lock-in effects for the Laschamp geomagnetic excursion recorded in the last glacial loess L1 of the Luochuan section (Zhu et al., 2006). Therefore, lock-in effects of geomagnetic reversals or excursions in Chinese loess are not pervasive and should be prudently evaluated.

A synthesis of previously published data on the geomagnetic polarities recorded in the CLP loess-paleosol sequence shows that the upper and lower boundaries of the Jaramillo subchron respectively occur in L10 and L12. The upper boundary of the Olduvai subchron is determined to be in the middle part of L25, and its lower boundary in the lower part of S26 or the uppermost part of L27 (Ding et al., 2002).

In addition to the major geomagnetic reversals, several geomagnetic excursions have been recorded in Chinese loess, such as Mono Lake, Laschamp, Norwegian-Greenland, Blake, Santa Rosa, Punaruu, Cobb Mountain, Gilsa and Reunion, among which the Blake excursion is the most widely recorded (Zhu et al., 1994, 1999; Zheng et al., 1995; Pan et al., 2002). However, the capability of recording short-lived geomagnetic excursions is variable and site-specific for Chinese loess. This characteristic is due to the complexity of the remanence acquisition, which is influenced by lock-in or smoothing effects (Zheng et al., 1995; Zhou and Shackleton, 1999; Wang et al., 2006), viscous overprinting of the remanence carried by coarse-grained magnetite of eolian origin (Wang et al., 2005b; Deng, 2008), and/or due to the episodic nature of loess accumulation during specific periods or in specific sections (Stevens et al., 2006; Zhu et al., 2007; Deng, 2008). As a result, geomagnetic excursions play only a limited role in the paleomagnetic dating of loess sediments.

The second category deals with the correlation between magnetic susceptibility variations of the CLP loess-paleosol sequence and marine oxygen isotope records. Heller and Liu (1982) first suggested a possible link between magnetic properties and paleoclimate recorded in the CLP loess-paleosol sequence. They further proposed that magnetic susceptibility variations of the sequence can be correlated with marine oxygen isotope records (Heller and Liu, 1984, 1986),

suggesting the close interdependence of the Chinese eolian deposits, the volume of land-based ice, and global climate, making the CLP loess-paleosol sequence one of the best terrestrial paleoclimatic archives. Subsequently, this correlation was further strengthened by a series of mineral-magnetic and non-magnetic proxies (Kukla et al., 1988; Hovan et al., 1989; Guo et al., 2000; Ding et al., 2002; Deng et al., 2006a; Hao et al., 2012). From the perspective of chronostratigraphy, the benchmark work of Heller and Liu (1984, 1986) serves as a milestone in global climatostratigraphy as well as an important step toward developing a high-precision chronology for the CLP loess-paleosol sequence.

The final category is pertinent to orbital tuning of paleoclimatic proxies. The establishment of a magnetochronostratigraphic framework and the correlation between magnetic susceptibility profiles and marine oxygen isotope records led to the use of the astronomical tuning approach as the basis for establishing high-resolution chronostratigraphies of the CLP loess-paleosol sequence. Ding et al. (1994) pioneered the application of the approach, yielding the first astronomically tuned timescale, named DYRL94, for the CLP loess-paleosol sequence. Subsequently, several improved astronomical timescales, such as LLZAD99 (Lu et al., 1999), HLD00 (Heslop et al., 2000), Chiloparts (Ding et al., 2002) and SCAY06 (Sun et al., 2006), have been established by tuning paleoclimatic proxy records (e.g., grain size and magnetic susceptibility) to theoretical changes in the elements of the Earth's orbit, taking into account the lock-in depth offsets of geomagnetic polarity reversals in loess and/or the lags between solar insolation forcing and the monsoon climate response. Significantly, the Chiloparts timescale (Ding et al., 2002) (Figure 1d) has been widely used and adopted by the Geologic Time Scale 2012 (Gradstein et al., 2012; Pillans and Gibbard, 2012), which was established using a stacked high-resolution grain size time series from five loess sections in the southern and middle CLP.

Constrained by those high-precision astronomical timescales, it is reasonable to conclude that for the CLP, loess-paleosol sequence units L0 and S0 correspond to the Holocene; units L1 and S1, to the Salawusuan Stage of the Upper Pleistocene; units from L2 to the upper part of L8, to the Zhoukoudianian Stage of the Middle Pleistocene; units from the middle-lower part of L8 to L33, to the Nihewanian Stage of the Lower Pleistocene; and units S33 and L34, to the Mazegouan Stage of the Upper Pliocene. In addition, the CLP loess-paleosol sequence yields plentiful mammalian faunas (Yue and Xue, 1996), such as the Longdan, Gongwangling, Yangguo, and Chenjiawo faunas (Table 1, Figure 2), whose chronologies have been well constrained by these accurate and precise timescales.

#### *4.1.2 Xiashu Loess*

A loess-paleosol sequence of eolian origin is distributed in the lower reaches of the Yangtze River, also named the Xiashu Loess. Previous investigations of the climatostratigraphy and magnetostratigraphy show that the Xiashu Loess was developed during Middle Pleistocene to Holocene time (Qiao et al., 2003; Wu et al., 2006; Zhang et al., 2009; Hao et al., 2010). Recently, the basal age of the Xiashu Loess was dated to ~0.9 Ma based on magnetostratigraphic and OSL chronologies of the Qingshan section in Yangzhou City and the Dagang borehole sequence in Zhenjiang City (Li et al., 2018) and of the Zhoujiashan section in Nanjing City (Wang et al., 2018). Therefore, the Xiashu Loess comprises a loess-paleosol sequence of the Holocene Series, the Salawusuan Stage (Upper Pleistocene) and the Zhoukoudianian Stage (Middle Pleistocene), and the uppermost Nihewanian Stage (Lower Pleistocene).

#### *4.1.3 Loess-paleosol sequences in other regions*

Loess-paleosol sequences are also well developed in other regions, such as eastern Inner Mongolia, the Kunlun Mountains in Xinjiang, western Sichuan Province, and south of the eastern Qinling Mountains. Chronologies of these sequences have been well constrained by the combination of magnetostratigraphy, OSL and TL dating, which have yielded a series of reliable basal ages for the sequences: e.g., 0.88 Ma in northern slope of the Kunlun Mountains (Fang et al., 2002); 1.22 Ma in Chifeng, eastern Inner Mongolia (Zeng et al., 2011, 2016); 1.1 Ma (Lu et al., 2007, 2011) and 1.2 Ma (Sun et al., 2017b), respectively, in Luonan Basin and Hanzhong Basin, eastern Qinling Mountains; and 1.16 Ma (Qiao et al., 2007) and 2.84 Ma (Qiao et al., 2015), respectively, in Ganzi and Jinchuan, western Sichuan Province.

### 4.2 Fluvio-lacustrine deposits

Quaternary fluvio-lacustrine strata are widely distributed in China. However, only a few sedimentary basins yield nearly continuous and long Quaternary fluvio-lacustrine sequences with reliable chronological constraints, such as the Nihewan and Sanmenxia Basins in northern China, the Yuanmou and Heqing Basins in Yunnan Province, southwestern China. In addition, the Yushe Basin in Shanxi Province, the Dali Basin in Yunnan Province and the Zanda Basin in Tibet Autonomous Region yield well developed Quaternary and Late Miocene to Pliocene fluvio-lacustrine strata. The chronostratigraphy of representative sedimentary basins is summarized in this section.

#### *4.2.1 Nihewan Basin*

The Nihewan Basin is in the transition zone between the North China Plain and the Inner Mongolian Plateau. The basin is filled with Late Neogene to Holocene lacustrine, fluvial and wind-blown deposits (Zhou et al., 1991; Zhu et al., 2001, 2003, 2004, 2007; Deng et al., 2008). The fluvio-

lacustrine sequence, which is overlain by Late Pleistocene or Holocene loess sediments and underlain by Late Neogene red clay of eolian origin, has been named "the Nihowan beds" (Barbour, 1924), namely the Nihewan beds. Today, this fluvio-lacustrine sequence is dissected in a southwest-northeast direction by the Sanggan River in the Yangyuan Basin and the Huliu River in the Yuxian Basin. The Nihewan beds are distributed in a series of sedimentary basins, including the Yangyuan, Huailai and Yuxian Basins in Hebei Province, the Datong and Tianzhen Basins in Shanxi Province, and the Yanqing Basin in Beijing. In particular, the Nihewan beds in Nihewan village, eastern Yangyuan Basin, are well developed, outcropping and rich in mammalian fossils.

The Nihewan Formation, which represents the type section of the Early Pleistocene in northern China (Young, 1950), was restricted to the lower portion of the Nihewan beds. Later, the name "Nihewan Formation" was used to define the entire fluvio-lacustrine sequence in the Nihewan Basin, that is, the Nihewan beds (Yuan et al., 1996; Deng et al., 2008). Usually, the Nihewan beds are subdivided into the Pliocene Daodi Formation, the Lower Pleistocene Nihewan Formation, the Middle Pleistocene Xiaodukou Formation, and the Upper Pleistocene Xujiayao Formation (Figure 3) (Zhou et al., 2000), which we follow here.

Considerable progress has been made during the past two decades in the magnetostratigraphic dating of the Nihewan Basin fluvio-lacustrine sequence and associated mammalian fossil localities and Paleolithic sites. Magnetobiostratigraphic results show that the sedimentary sequence spans the interval from the late Gauss chron, through the Matuyama chron, including the Jaramillo and Olduvai normal subchrons, to the Brunhes chron. In addition, several fine-scale features of the magnetostratigraphy are recorded in the sequence, such as the Kamikatsura, Santa Rosa, Punaruu, Cobb Mountain and Reunion geomagnetic excursions (Zhu et al., 2004; Wang et al., 2005a; Deng et al., 2006b; Liu et al., 2012). Therefore, the basal age of the Nihewan beds, at least in the eastern Nihewan Basin, is constrained to the Late Pliocene (Liu et al., 2012).

In natural outcrops of several representative sections, the basal ages of the Nihewan beds range from Late Pliocene to early Middle Pleistocene, possibly due to local faulting activity or geomorphological location (e.g., ~3 Ma at Xiashagou (Liu et al., 2012), ~2 Ma at Dachangliang (Deng et al., 2006b), ~2 Ma at Taiergou (Wang et al., 2004), ~1.7 Ma at Haojiatai-Majuangou (Zhu et al., 2004), ~1.5 Ma at Xiaochangliang (Zhu et al., 2001), ~1.2 Ma at Feiliang (Deng et al., 2007b), ~1.1 Ma at Donggutuo (Wang et al., 2005a), ~0.8 Ma at Hougou (Zuo et al., 2012), and <0.78 Ma at Hutouliang). The Xiashagou section is of special significance for chronostratigraphic investigations of fluvio-lacustrine strata in northern China because it has yielded the classical Xiashagou fauna, also named the Nihewan fauna (*sensu stricto*) (Teilhard de Chardin and Piveteau, 1930), the almost complete Nihewan beds over the last ~3 million years, as well as the Pliocene-Pleistocene boundary (Liu et al., 2012). The Nihewan beds are rich in mammalian fossils, known as the Nihewan faunas (*sensu lato*). Chronologies of the faunas are discussed in Section 3.1.

Th top of the Nihewan beds is diachronous. Considering that the Late Pleistocene loess sediments (e.g., at the Haojiatai, Xiaochangliang, Donggutuo and Hougou sections) or Holocene soil (e.g., at the Huabaogou, Hongya and Hutouliang sections) were found to overlie the fluvio-lacustrine successions, Deng et al. (2008) suggested that drying up of the Nihewan paleolake commenced during the last interglacial period (e.g., at the Haojiatai and nearby sections) and that the ultimate disappearance of the paleolake probably occurred during the late last glaciation (e.g., at the Hongya, Huabaogou and Hutouliang sections).

Soon after, OSL chronologies provided more accurate and precise constraints on the ages of the last interglacial soil and the uppermost Nihewan beds. For example, the bottom of S1 at the Haojitai section is dated to 127.5±6.6 ka (Zhao et al., 2010) or ~130 ka (Nian et al., 2013); and the top of the Nihewan beds is dated to 266±16 ka (Zhao et al., 2010) or 420−360 ka (Nian et al., 2013) at the Haojitai section, 420−360 ka (Nian et al., 2013) at the Hougou and Hongya sections, and ~270 ka at the Hutouliang section (Nian et al., 2013). The Nihewan beds were more-or-less eroded before the onset of loess sediment accumulation in the Nihewan Basin, and thus sediment accumulation of the Nihewan beds may have terminated in the late Middle Pleistocene (e.g., roughly at 300−200 ka), corresponding to the period of formation of paleosols S2−S3 in the Chinese Loess Plateau.

Considering all the available evidence, it is reasonable to conclude that for the Nihewan beds the Daodi Formation in the lowermost part corresponds to the Mazegouan Stage of the Upper Pliocene; the Nihewan Formation in the lower part, to the Nihewanian Stage of the Lower Pleistocene; the Xiaodukou Formation in the middle part, to the Zhoukoudianian Stage of the Middle Pleistocene; and the Xujiayao Formation in the upper part, to the Salawusuan Stage of the Upper Pleistocene.

#### *4.2.2 Sanmenxia Basin*

The Sanmenxia Basin, located in the middle reaches of the Yellow River, yields a fluvio-lacustrine sequence of the Plio-Pleistocene period, with a thickness of ~300 m. The sedimentary sequence, named the Sanmen Series by Professor Ding Wenjiang in 1918 (Pei and Huang, 1959) and now collectively called the Sanmen Formation (Zhou et al., 2000), is distributed in the valleys of the Yellow River, the Wehe River and their tributaries in Shaanxi, Shanxi and Henan provinces (Wang et al., 2002).

Over the past century, intensive studies of stratigraphic subdivision and chronology were carried out on the Sanmen Formation. The latest magnetostratigraphic investigations coupled with TL dating carried out on the Huangdigou section (~280 m thick) in Pinglu County, Shanxi Province (Wang et al., 2002) place stringent age controls on the Sanmen Formation sedimentary sequence. The results show that the Huangdigou section spans the interval from chron C3n.3n (Sidufjall, 4.896−4.799 Ma) to chron C1n (Brunhes).

Constrained by Wang et al.'s (2002) chronologies for the Huangditou section, the M-B and G-M boundaries were placed at depths of 73 m and 188 m, respectively. The onset of basin deposition occurred at ~5.4 Ma. The presence of the Biwa geomagnetic excursion recorded ~5 m below the top of the fluvio-lacustrine Sanmen Formation, and the TL age of 148 ka obtained from the bottom of loess sediments overlying the third terrace of the Yellow River near Huangdigou, suggest that deposition in the basin terminated at ~0.15 Ma.

The upper part of the Sanmen Formation was informally called the yellow Sanmen Formation, and the lower part the green Sanmen Formation (Yuan and Du, 1984; Zhou et al., 2000). Xue (1981) found the Youhe fauna in the upper part of the green Sanmen Formation and established the Youhe Formation. The age of the Youhe Formation was estimated to be Late Pliocene in terms of its biostratigraphy (Yuan and Du, 1984). Thus, the yellow and green Sanmen Formations correspond roughly to the Pleistocene and Pliocene, respectively.

The Sanmen Formation is rich in mammalian fossils with ages ranging from Pliocene to Middle Pleistocene (Pei and Huang, 1959). However, the exact stratigraphic position of each faunal element is unknown. Therefore, high-resolution magnetostratigraphic investigations coupled with biostratigraphy are needed to precisely constrain the ages of the Sanmen Formation and associated mammalian faunas.

#### *4.2.3 Yushe Basin*

The Yushe Basin yields a fluvio-lacustrine sequence of the period from the Late Miocene to Quaternary, with a thickness of about 800 m, collectively named the Yushe Group (Qiu et al., 1987); it is well developed in Yushe and Wuxiang Counties, southeastern Shanxi Province. The basin consists of five sub-basins, including the Yuncu, Nihe, Ouniwa, Tancun and Zhangcun, among which the Yuncu and Zhangcun sub-basins yield nearly continuous and fossiliferous sedimentary sequences (Qiu et al., 1987; Shi et al., 1993; Tedford et al., 2013).

The Yushe Group in the Zhangcun sub-basin consists of the Renjianao and Wangning formations of the Lower Pliocene, the Zhangcun Formation of the Upper Pliocene, and the Louzeyun Formation of the Lower Pleistocene (Shi et al., 1993; Li et al., 2004c). The Yushe Group in the Yuncu sub-basin consists of the Mahui Formation of the Upper Miocene, the Gaozuang Formation of the Lower Pliocene, the Mazegou Formation of the Upper Pliocene, and the Haiyan Formation of the Lower Pleistocene (Qiu et al., 1987; Tedford et al., 2013). The fluvio-lacustrine sedimentary sequence in the Yuncu sub-basin is of special significance because it is rich in mammalian fossils and yields type sections of the Gaozhuangian Stage of the Lower Pliocene and the Mazegouan Stage of the Upper Pliocene for Chinese terrestrial strata (Deng et al., 2010; Deng and Hou, 2011).

Magnetostratigraphic results show that the Haiyan Formation in the Yuncu sub-basin is of early Matuyama (chron C2r) age (Tedford et al., 1991). Later, magnetostratigraphic results showed that the Louzeyu Formation in the Zhangcun sub-basin spans the interval from chron C2r to early chron C1r.2r, and that the G-M geomagnetic reversal is in its uppermost part (Shi et al., 1993). Thus, the Louzeyu Formation in the Zhangcun sub-basin and the Haiyan Formation in the Yuncu sub-basin can be constrained to the Nihewanian Stage of the Lower Pleistocene.

#### *4.2.4 Yuanmou Basin*

The Yuanmou Basin in Yunnan Province, southwestern China, yields a fluvio-lacustrine sequence dating to the interval from the Late Miocene to the Early Pleistocene, with a thickness of about 700 m. The sedimentary sequence is rich in mammalian fossils and yields a type section of the Lower Pleistocene fluvio-lacustrine strata in southern China.

In 1938, Bien conducted geological surveys in the Yuanmou Basin, and later named the sequence "the Yuanmo beds", namely the Yuanmou beds. Bien (1940) further suggested that the Yuanmou beds are of Late Pliocene (Villafranchian) in age. Later, the sequence was named the Yuanmou Formation, which was included in the Chinese Regional Stratigraphic Chart (Draft) and suggested to be Early Pleistocene in age (Editorial Board of Chinese Geology, Institute of Geology of Academia Sinica, 1956).

Chou (1961) subdivided the above-mentioned Yuanmou Formation into two parts: the lower one being the Shagou bed, which bears fossil *Enhydriodon falconeri* and is suggested to be of Late Pliocene in age; and the upper one the Quaternary bed bearing fossils of *Equus*, Bovinae and Cervidae, which is suggested to be Early Pleistocene in age and corresponding to the Nihewan beds in northern China.

In 1965, Qian Fang found two incisors of *Homo* near Shangnabang village. From 1965−1977, Qian and his colleagues made a systematic study of the Yuanmou Basin sedimentary sequence, collectively called the Yuanmou Formation (Qian and Zhou, 1991). They established an integrative stratigraphic framework for the sequence based on investigations of lithostratigraphy, biostratigraphy and magnetostratigraphy (Qian and Zhou, 1991). The Yuanmou Basin sequence consists of 4 lithologic members (M1−M4) and 28 lithologic beds (Beds 1−28), from oldest to youngest:

M1 (Beds 1−4), M2 (Beds 5−13), M3 (Beds 14−23) and M4 (Beds 24−28), which was paleomagnetically dated to 3.1−1.5 Ma (Pu and Qian, 1977), and then was revised to 3.40−1.33 Ma (Qian and Zhou, 1991).

Zhang et al. (1994) collectively called the Yuanmou Basin sedimentary sequence the Yuanmou Group, and further subdivided the strata into two parts: the lower part being the Shagou Formation, corresponding to the Shagou bed named by Chou (1961); and the upper part, the Yuanma Formation.

Currently, there is a consensus that the Yuanmou Basin sedimentary sequence consists of two formations: the lower one being the Shagou Formation; and the upper one the Yuanmou Formation (Figure 3) (Zhou et al., 2000), as initially suggested by Chou (1961).

The chronology of the Yuanmou Basin sedimentary sequence has been intensively studied using magnetostratigraphy (e.g., Li et al., 1976; Pu and Qian, 1977; Qian and Zhou, 1991; Zhu et al., 2008a, 2008b). Up to now, the most high-resolution magnetostratigraphy of the sequence, which is based on Qian and Zhou's (1991) lithostratigraphic framework, was obtained by Zhu et al. (2008a, 2008b) through magnetostratigraphic investigations of the sections of Gantang-Maoyi, Dapoqing and Niujianbao, which spans the interval from chron C3n.3r (4.997−4.896 Ma) to chron C1r.2r (1.778−1.072 Ma) with an age range of 4.9−1.4 Ma for the sequence.

Constrained by Zhu et al.'s (2008a, 2008b) magnetochronology, the M1-M2 boundary is placed in middle chron C2An.2n (3.207−3.116 Ma), and is dated to ~3.2 Ma; the M2-M3 boundary (namely the boundary between the Shagou Formation and the overlying Yuanmou Formation) is placed roughly 20 m below the Reunion geomagnetic excursion, and is dated to ~2.2 Ma; and the M3-M4 boundary is placed at the lower boundary of the Olduvai subchron, and is dated to ~2.0 Ma.

As a result, the age of the Shagou Formation can be paleomagnetically estimated to be 4.9−2.2 Ma, and is constrained to an interval from the Gaozhuangian Stage of the Upper Pliocene to the Nihewanian Stage of the Lower Pleistocene. The age of the Yuanmou Formation can thus be paleomagnetically estimated to be 2.2−1.4 Ma, and is constrained to the Nihewanian Stage. The Yuanmou fauna bearing *Equus yunnanensis* occurs in the Yuanmou Formation and in a stratigraphic interval from Bed 18 of the middle part of M3 and Bed 27 of the upper part of M4 (Qian and Zhou, 1991) and has an estimated age of 2.1−1.5 Ma. The mammalian assemblage of the Yuanmou fauna is similar taxonomically to the Nihewan fauna in northern China and the Villafranchian fauna in Europe (Bien, 1940; Pei, 1961).

#### 4.2.5 *Heqing Basin*

The Heqing Basin in Yunnan Province, southwestern China, yields a lacustrine sequence of the interval from the Late Pliocene to the Late Pleistocene. The Heqing drill core (An et al., 2011) obtained in 2002 yielded a sequence of clays and clayey silts. The initial drilling depth is 737.72 m, and the calibrated sedimentary depth is 665.83 m. The magnetostratigraphy of the Heqing borehole sequence was described in detail by An et al. (2011) and is summarized here.

Paleomagnetic measurements of U-channel samples show that the Heqing Basin sequence spans the interval from the late Gauss chron (C2An.1n) to the late Brunhes chron (C1n). In addition, the sequence records several short intervals of possible transitional field behavior, such as the Laschamp, Santa Rosa, Gardar and Gilsa geomagnetic excursions. The M-B and G-M boundaries were placed at depths of 152.00 m and 614.47 m, respectively. The onset of basin deposition occurred at 2.78 Ma. The presence of the Laschamp geomagnetic excursion in the depth interval of 4.37−4.59 m suggests that deposition in the basin terminated during late Late Pleistocene.

Based on An et al.'s (2011) magnetochronology, the infilling of Heqing Basin can be constrained to an interval from the Mazegouan Stage of the Upper Pliocene to the Salawusuan Stage of the Upper Pleistocene, and the major part of the deposition comprises the complete sedimentary sequence of the Nihewanian Stage (Lower Pleistocene) and the Zhoukoudianian Stage (Middle Pleistocene).

#### 4.2.6 *Dali Basin*

The Dali Basin in Yunnan Province, southwestern China, yields a fluvio-lacustrine sequence spanning the interval from the terminal Miocene to the Early Pleistocene, with a thickness of up to 1000 m. The sedimentary sequence, named the Sanying Formation, and bearing the Sanying Flora of Pliocene age, mainly consists of lacustrine, fluvial, alluvial and swamp deposits.

Li et al. (2013) divided the Dali Basin sequence into four facies associations (FA), consisting of, from oldest to youngest, swamp coal-bearing clays interbedded with fluvial sands (FA1, ~295 m thick); fluvial or lacustrine sands and silts (FA2, ~195 m thick); lacustrine clays and silts with interbeds of conglomerates and sands (FA3, ~260 m thick); and alternating conglomerates and sands of fluvial and alluvial facies (FA4, ~215 m thick).

Magnetostratigraphic investigations of the Dasongping section show that the sequence spans the interval from chron C4n.1r (7.695−7.642 Ma) to chron C2n (1.945−1.778 Ma) with an age range of 7.6−1.8 Ma for the sequence (Li et al., 2013). The age of the Dali Basin sedimentary sequence can thus be paleomagnetically constrained to an interval from the Late Miocene to the Early Pleistocene.

Constrained by the magnetochronology of Li et al. (2013), Unit FA1 corresponds to the interval from the upper Bahean Stage (Upper Miocene) to the lower Baodean Stage (Upper Miocene); Units FA2 and FA3, which comprise the main part

of the Sanying Formation, correspond to the interval from the upper Baodean Stage (Upper Miocene), through the Gaozhuangian Stage (Lower Pliocene), to the Mazegouan Stage (Upper Pliocene); and Unit FA4 corresponds to the interval from the upper Mazegouan Stage (Upper Pliocene) to the lower Nihewanian Stage (Lower Pleistocene). The Plio-Pleistocene boundary, roughly corresponding to the G-M boundary, is in the lower part of Unit FA4, ~30 m above the FA3-FA4 boundary.

#### *4.2.7 Zanda Basin*

The Zanda Basin in the southwestern margin of the Tibetan Plateau yields a sedimentary sequence of fluvial, lacustrine, eolian and alluvial fan deposits with a thickness of ~800 m, which is collectively named the Zanda Formation (Wang et al., 2013b). The lower part, ~200-m thick, consists mainly of fluvial conglomerates and conglomeratic sands; the middle part, ~250-m thick, is mainly composed of lacustrine claystones interbedded with sands; and the upper part, ~350-m thick, mainly comprises alluvial conglomerates interbedded with fluvial claystones. Fossil mammals are mainly preserved in the middle part of the Zanda Formation at about the 170−600 m level, and fossil localities above the 620-m level are fewer (Wang et al., 2013b).

Magnetostratigraphic investigations carried out on the Zanda Formation sedimentary sequence by several research groups yielded diverse magnetochronologies (Qian, 1999; Wang et al., 2008; Saylor et al., 2009). Basal ages of the basin infilling range from 9.5−6.15 Ma, with termination ages from 2.6 Ma to less than 1 Ma.

Wang et al. (2013b) synthesized the biostratigraphic data and magnetic stratigraphies of Qian (1999), Wang et al. (2008) and Saylor et al. (2009). Wang et al.'s (2013b) reinterpretation of the magnetobiochronology shows that the Zanda Formation spans the interval from chron C3An.1r (6.436−6.252 Ma) to chron C1n (Brunhes) with an age range 6.4−0.4 Ma for the sequence. The age of the Zanda Basin sedimentary sequence can thus be paleomagnetically constrained to an interval from the Late Miocene to Middle Pleistocene.

The magnetobiochronology synthesized by Wang et al. (2013b) provides reliable age constraints for the Zanda Formation. The lower part at the 0−152-m level, bearing fossil *Hipparion,* is dated to extend from 6.4−5.3 Ma, corresponding to the Baodean Stage of the Upper Miocene. The middle part at the 152−620-m level is dated to extend from 5.3−2.6 Ma, corresponding to the Gaozhuangian and Mazegouan Stages of the Pliocene. The upper part at the 620−800-m level is dated to extend from 2.6−0.4 Ma, corresponding to the Nihewanian Stage (Lower Pleistocene) and Zhoukoudianian Stage (Middle Pleistocene). The G-M and M-B boundaries are placed at the levels of 620 m and 744 m, respectively. Fossil *Equus* with an estimated age 2.48 Ma is found to be just above the G-M boundary.

#### *4.2.8 Other sedimentary basins*

Other sedimentary basins also yield well-developed Quaternary strata. For example, biostratigraphic analyses suggest that the Qigequan Formation in the Qaidam Basin, northern Tibetan Plateau, roughly corresponds to the Nihewanian Stage (Wang et al., 2007b). The lithostratigraphy, biostratigraphy and magnetic stratigraphy of seven drill cores from the Yinchuan Basin, in the middle reaches of the Yellow River, suggest that the Yinchuan Formation roughly corresponds to the Nihewanian Stage (Tong et al., 1998). The magnetostratigraphy of the Yilangjian borehole sequence in Qinghai Lake, northeastern Tibetan Plateau, suggests that the ~400-m-thick upper and middle parts have a nearly complete Quaternary lacustrine sequence (Fu et al., 2013). Magnetostratigraphic investigations show that the Quaternary sedimentary sequence of fluvial, lacustrine and alluvial fan deposits in the North China Plain has a thickness of ~300−500 m (Liu et al., 2010b; Yuan et al., 2014). In addition, chronologies of the widely distributed lacustrine sequences (including Maar lake deposits) since the Late Pleistocene (especially since the Last Glacial Maximum) are beyond the scope of this study.

### 4.3 Red soil sequence in southern China

A paleosol unit characterized by red and white veins, which is widely distributed in the subtropical and tropical southern China, is usually referred to as a vermiculated red soil (Yin and Guo, 2006) or red soil sequence (Yuan et al., 2008). The parent materials of the red soil sequence are usually of eolian (Qiao et al., 2003) or fluvial (Hou et al., 2000) origin. Magnetostratigraphic investigations show that the red soil sequence in the middle and lower reaches of the Yangtze River began to accumulate during the late Matuyama reversed chron (that is, the late Early Pleistocene) (Jiang et al., 1997; Zhao et al., 2007; Liu et al., 2008) or just prior to the M-B geomagnetic reversal (that is, the terminal Early Pleistocene) (Qiao et al., 2003). Most of the studied sections record the M-B geomagnetic reversal. In addition, some of the sections record the Jaramillo normal subchron (e.g. the Qiliting section in Zhejiang Province (Liu et al., 2008), the Changhongdadao section in Jiangxi Province (Jiang et al., 1997), and the Shengli and Huangjia sections in Sichuan Province (Zhao et al., 2007)). Therefore, the basal age of the red soil sequence in the middle and lower reaches of the Yangtze River, in the northern part of subtropical southern China, can be constrained to as early as ~1.2 Ma.

In addition, the Bose Basin in Guangxi Zhuang Autonomous Region, which is close to the Tropic of Cancer, yields a well-developed red soil sequence. However, strong chemical weathering occurring under subtropical climatic conditions

in the Bose Basin has resulted in a chemical remanent magnetization (CRM) overprint that is sufficiently strong to mask the primary natural remanent magnetization (NRM) (Deng et al., 2007a; Liu et al., 2010a). As a result, the red soil sequence in the Bose Basin has failed to faithfully record past geomagnetic field behavior, and magnetostratigraphy cannot be used to date the sequence. Fortunately, the middle to upper parts of the red soil sequence in the Bose Basin yield Australasian tektites, which have been precisely dated to 803 ±3 ka by $^{40}Ar/^{39}Ar$ analyses (Hou et al., 2000), just prior to the M-B geomagnetic reversal. Therefore, the red soil sequence in the Bose Basin began to accumulate at least during the terminal Early Pleistocene.

It should be noted that the age of vermiculation of the red soil sequence in southern China is significantly later than that of sediment accumulation. By combining analyses of climatostratigraphy and soil micromorphology and mineralogy, Yin and Guo (2006) determined that the timing of the vermiculation for the red soil sequence in southern China corresponds to the period of formation of paleosols S4 and S5 in the Chinese Loess Plateau, ~0.6−0.4 Ma (Ding et al., 2002).

Considering all the available chronological evidence, it can be concluded that the red soil sequence in southern China corresponds to the upper part of the Nihewanian Stage and the lower part of the Zhoukoudianian Stage.

### 4.4 Cave and fissure deposits and associated faunas in southern China

The Pleistocene mammalian fossils in southern China, often preserved in karstic caves or fissures, are generally known as the *Ailuropoda-Stegodon* fauna. With an increasing number of cave/fissure localities being discovered, detailed investigations on the unearthed mammalian fossils suggest that *Gigantopithecus blacki* can be regarded as an appropriate chronospecies of the Early Pleistocene mammalian assemblage. Thus, the mammalian fauna bearing *Gigantopithecus blacki* is named the *Gigantopithecus* fauna (Chou, 1957; Jin et al., 2008). The terms "*Gigantopithecus* fauna" and "*Ailuropoda-Stegodon* fauna" were widely used in Quaternary biostratigraphic investigations, and were regarded as typical mammalian faunas of the Early and Middle Pleistocene, respectively (Yuan and Du, 1984).

Biochronology has long been used to determine the ages of the cave/fissure faunas. Considerable progress has been made during the past decade in dating the cave/fissure sedimentary sequences and associated mammalian faunas using magnetostratigraphy, U-series, and/or ESR. The resulting age data provide insights into our understanding of the temporal and spatial distribution of the *Gigantopithecus* and *Ailuropoda-Stegodon* faunas in southern China. Based on these age data, Wang et al. (2014) modified the *Gigantopithecus* fauna to the *Gigantopithecus-Sinomastodon* fauna to distinguish the latter from the typical Middle Pleistocene *Ailuropoda-Stegodon* fauna and the Late Pleistocene Asian elephant fauna. Most of the localities yielding the *Gigantopithecus-Sinomastodon* fauna are in Guangxi, and others are distributed in the Guizhou, Hainan, Hubei and Chongqing regions of southern China. Based on updated geochronological and biochronological data, the evolutionary processes of the *Gigantopithecus-Sinomastodon* fauna can be divided into four stages, as follows (Jin et al., 2014; Wang et al., 2017) (Figure 2).

The first stage is the early period of the Early Pleistocene, corresponding to the early Matuyama reversed chron (C2r) with an age range of 2.58–1.95 Ma. The representative faunas of this stage include those from Baikong Cave (2.58–1.95 Ma) in the Chongzuo area (Guangxi) (Sun et al., 2014), Longgupo (2.5–2.2 Ma) in Wushan (Chongqing) (Han et al., 2017) and Liucheng Juyuan Cave (Guangxi), which contain *Gigantopithecus blacki* with a relatively small dental size, some Neogene survivors and taxa which first appeared during the Pleistocene (Jin et al., 2014; Wang et al., 2017). The age of the Liucheng Juyuan Cave fauna was determined to be 1.21–0.94 Ma based on the combination of ESR and U-series dating (Rink et al., 2008); however, biochronologic evidence suggests that the fauna, which is comparable with the faunas of Baikong Cave and Longgupo in age and serves as a representative of the *Gigantopithecus-Sinomastodon* fauna, should be assigned to the early Early Pleistocene (Jin et al., 2014).

The second stage is the middle period of the Early Pleistocene, ranging from the onset of the Olduvai normal subchron to the Cobb Mountain geomagnetic excursion (1.95–1.20 Ma). The representative faunas of this stage include those from Chuifeng Cave (1.92±0.14 Ma) (Shao et al., 2014) and Mohui Cave (1.95–1.78 Ma) (Sun et al., 2017a) in Bubing Basin (Guangxi), as well as those from Chongzuo Juyuan Cave (1.95–1.78 Ma) (Sun et al., 2014) and Sanhe Cave (~1.2 Ma) (Jin et al., 2009; Sun et al., 2014) in the Chongzuo area (Guangxi). The faunas possess transitional features implied by the increased body size of some species, the disappearance of primitive species and the first appearance of some newcomers (Jin et al., 2014; Wang et al., 2017).

The third stage is the late period of the Early Pleistocene, corresponding to the interval from the termination of the Cobb Mountain geomagnetic excursion to the M-B geomagnetic reversal (1.20–0.78 Ma). The Queque Cave fauna (1.07–0.99 Ma) (Sun et al., 2014) in the Chongzuo area (Guangxi) serves as a representative of this stage, which reveals distinctly increased dental dimensions of some taxa, such as *Gigantopithecus blacki*, *Ailuropoda* and *Tapirus* (Jin et al., 2014). The *Gigantopithecus-Sinomastodon* fauna in this stage yields several features (e.g. a decreasing proportion of Neogene survivors, the appearance of some species that are common during the Middle Pleistocene and the co-

existence of typical species of the Early and Middle Pleistocene (Jin et al., 2014)) that imply a transitional nature of the fauna, from the Early to Middle Pleistocene.

The last stage is the early to middle period of the Middle Pleistocene with an age range of 0.78–0.32 Ma. The Hejiang Cave fauna (400–320 ka) in the Chongzuo area (Guangxi) (Zhang et al., 2014) serves as a representative of this stage, which is similar in age to the Tham Khuyen Cave fauna (475 ±125 ka) in northern Vietnam (Ciochon et al., 1996). These faunas are characterized by a higher proportion of extant species and the replacement of Early Pleistocene taxa by typical Middle Pleistocene taxa (Wang et al., 2017).

In addition to the sites bearing the *Gigantopithecus-Sinomastodon* fauna described above, several important sites bearing the *Stegodon-Ailuropoda* fauna in southern China have been precisely dated due to the rapid development and wide application of geochronological techniques. For example, coupled ESR and U-series dating methods successfully provided a chronological sequence of faunas in the Bubing Basin, Guangxi Province, including Shizi Cave (0.517–0.366 Ma) (Kong et al., 2012), Wuyun Cave (0.35–0.20 Ma, Wang et al., 2007 or 0.279–0.076 Ma, Rink et al., 2008), Upper Pubu Cave (0.28–0.088 Ma) (Rink et al., 2008) and Luna Cave (0.127–0.07 Ma) (Bae et al., 2014). In addition, Liu et al. (2015) reported a cosmogenic $^{26}Al/^{10}Be$ burial age of 0.76±0.06 Ma for Bailong Cave in Yunxian, Hubei Province; and the age of the Dadong Cave fauna in Panxian, Guizhou Province was well constrained by OSL dating to 300–190 ka (Zhang et al., 2015).

In particular, two fossil sites in Guangxi, Bulali Hill in Wuming and Black Cave in Daxin, yield both the *Gigantopithecus-Sinomastodon* fauna and the *Ailuropoda-Stegodon* fauna. Rink et al. (2008) analyzed biochronologies of the two faunas based on their faunal assemblages, and further obtained ages of the two localities (380–308 ka for Daxin and 745–481 ka for Wuming) based on ESR model ages and/or coupled ESR/$^{230}Th/^{234}U$ ages. However, the exact stratigraphic position of each faunal element is unknown because the two localities were discovered and excavated several decades ago. Therefore, it is difficult to assign precise ages to the *Gigantopithecus* fauna and the *Ailuropoda-Stegodon* fauna at Wuming and Daxin. Jin et al. (2009) suggested the *Gigantopithecus* fauna of the Black Cave in Daxin is older than that of Bulali Hill in Wuming based on biochronological data. Recently, the *Ailuropoda-Stegodon* fauna of Black Cave was dated to 383±20 ka by U-series and ESR/U-series dating (Shao et al., 2017). This finding further implies that the *Gigantopithecus* fauna in this locality at a lower stratigraphic position should be older than 400 ka (Shao et al., 2017).

The chronological sequence of these faunas suggests that since the early-middle periods of the Middle Pleistocene, the *Ailuropoda-Stegodon* fauna gradually flourished while the *Gigantopithecus-Sinomastodon* fauna began to decline in southern China. From the perspective of Quaternary land mammal ages/stages in China, the *Gigantopithecus-Sinomastodon* fauna existed from the Nihewanian Age of the Early Pleistocene to the middle Zhoukoudianian Age of the Middle Pleistocene, while the *Ailuropoda-Stegodon* fauna flourished during the middle-late Zhoukoudianian Age and lasted until the Salawusuan Age of the Late Pleistocene.

### 4.5 Cave stalagmites

Since the 1980s, the development and application of high-precision U-Th isotopic measurements by thermal ionization mass spectrometry (TIMS) (Edwards et al., 1987), inductively coupled plasma-mass spectrometry (ICP-MS) (Luo et al., 1997; Shen et al., 2002) and multi-collector inductively coupled plasma mass spectrometry (MC-ICP-MS) (Cheng et al., 2013) have led to the establishment of high-precision timescales for stalagmite records worldwide. Those pioneering achievements have substantially contributed to research progress in global climate change and the climatostratigraphy of the late Quaternary. During the past two decades, multiple high-resolution oxygen isotope records, especially from Chinese caves, have been established, which are constrained by high-precision U-Th chronologies. The representative records include those from Nanjing Hulu Cave (Nanjing, Jiangsu Province), Sanbao Cave (Mt. Shennongjia, Hubei Province) and Dongge Cave (Guizhou Province). The records are an important step toward establishing a Chinese benchmark of late Quaternary climate changes based on oxygen isotope records of stalagmites.

As a hallmark of the research into Chinese stalagmites, the $\delta^{18}O$ record from Hulu Cave unambiguously documents East Asian monsoonal variability during the last glacial period (75−11 ka) (Wang et al., 2001). Subsequently, the stalagmite $\delta^{18}O$ records from Sanbao and Dongge Caves extended the high-resolution $\delta^{18}O$ records of the East Asian monsoon back to the last interglacial period (Yuan et al., 2004), the penultimate interglacial period (Wang et al., 2008), and the ends of the third- and fourth-most recent ice ages (Cheng et al., 2009). Most recently, Cheng et al. (2016) successfully extended the stalagmite $\delta^{18}O$ record from Sanbao Cave to the ends of the fifth- and sixth-most recent ice ages, which cover the entire range of uranium/thorium dating. These stalagmite $\delta^{18}O$ records meticulously depict orbital to suborbital climate variations with high-resolution time series for the past seven glacial-interglacial cycles, and demonstrate that insolation changes caused by the Earth's precession cycle drove these ice age terminations (Cheng et al., 2016).

### 4.6 Marine deposits

Quaternary marine deposits in China mainly include detrital

and biogenic reef sediments in the South China Sea, and detrital sediments on the continental shelves of eastern China. The latter are of both marine and continental origin and are described in this section.

#### *4.6.1 Marine detrital sediments in the South China Sea*

Detrital sediments are mainly distributed in the Zhujiangkou Basin of the northern South China Sea and in the South China Sea Basin. The Pleistocene sedimentary sequence in the Zhujiangkou Basin consists of gray and grayish-green clays intercalated with thin-bedded silts, which are of marine origin. Based on their characteristic calcareous nannofossil assemblage, the base of the sequence can be correlated to Zone NN18 of the calcareous nannofossil zonation, close to the base of the Quaternary (Huang, 1997).

The South China Sea Basin consists of northern and the southern sub-basins. Systematic studies, including lithostratigraphy, biostratigraphy, and carbon and oxygen isotope stratigraphies of sediment cores recovered during ODP Leg 184, have led to the establishment of a chronostratigraphic framework for the northern sub-basin (Wang et al., 2003). The detrital sediments in the northern sub-basin contain pelagic silts and clays, which are intercalated with sandy and gravel layers and are rich in biogenic debris. Importantly, the marine $\delta^{18}$O record from ODP Site 1148 spans the interval from the Late Oligocene to the Quaternary (Wang et al., 2003), and that from the ODP Site 1143 provides one of the highest-resolution $\delta^{18}$O records since the Pliocene (Tian et al., 2002). Additionally, the depositional characteristics of the sedimentary sequence in the southern sub-basin resemble those of the northern sub-basin, but they are less well studied.

Tektite-bearing layers and volcanic ash layers facilitate regional stratigraphic correlation in the South China Sea Basin. The tektites were found at the depth interval of 0.58−1.09 m below the M-B boundary at ODP Hole 1146B near the continental slope of the northern South China Sea (Li et al., 2004b), and at the depth interval of 7.80−8.10 m in core SO95-17957-2 from the northern Nansha area, corresponding to MIS 19/20 transition (Zhao et al., 1999). These South China Sea tektites as well as the Bose tektites most probably belong to the tektites of the Australasian strewn field (Zhao et al., 1999; Hou et al., 2000; Li et al., 2004b), with the latter being precisely dated to 803±3 ka by $^{40}$Ar/$^{39}$Ar analyses (Hou et al., 2000).

Three volcanic ash layers of about 2-cm-thick have been identified in the upper part of the ODP Hole 1143A, at depths of 5.55 m (Layer A), 42.66 m (Layer B), and 48.25 m (Layer C) (Liang et al., 2001). Major element analyses using an electron microprobe analyzer led the authors to suggest that the three volcanic ash layers most likely come from the Quaternary Toba volcanic eruptions in the northern Sumatra, Indonesia, and that Layers A, B and C respectively correspond to the YTT (Young Toba Tuff), OTT (Old Toba Tuff) and HDT (Haranggoal Dacite Tuff). Moreover, the ages of the three ash layers were estimated to be 0.07, 0.80 and 1.0 Ma, respectively, based on microbiostratigraphy (Liang et al., 2001). These age estimates of Layers A, B and C are consistent with $^{40}$Ar/$^{39}$Ar ages of the YTT (73.7±0.3 ka) (Mark et al., 2017), OTT (792.4±0.5 ka for OTTA and 785.6 ±0.7 ka for OTTB) (Mark et al., 2017), and HDT (ca. 1.2 Ma) (Chesner and Rose, 1991).

#### *4.6.2 Biogenic reefs in the South China Sea*

Biogenic reefs have developed from Neogene to Quaternary time, mainly on carbonate platforms of the Xisha, Zhongsha and Nansha Islands. As the most representative biogenic reefs in the South China Sea, the biogenic reef sequence of the Xisha Islands can be divided into five formations, from oldest to youngest: the Sanya Formation (roughly Lower Miocene), the Meishan Formation (roughly Middle Miocene), the Huangliu Formation (roughly Upper Miocene), the Yinggehai Formation (roughly Pliocene), and the Quaternary Ledong Formation (Shao et al., 2016). The base of the Ledong Formation was placed at the exposure surface of 215-m-depth based on sequence stratigraphic analyses of the Xike-1 borehole sequence drilled from the northern Xisha Islands (Zhu et al., 2015a). Subsequently, $^{230}$Th dating of the biogenic reefs yielded an age of 151±1 ka at 32.7-m depth (Wang et al., 2017). In addition, magnetostratigraphic investigations indicate that the M-B boundary is located at the depth of 65 m, and that the base of the Ledong Formation roughly corresponds to the lower boundary of the Olduvai normal subchron with an age of ~2.0 Ma. Constrained by the chronologies, the upper 30-m of the Xike-1 borehole sequence belong to the Salawusuan Stage; the depth interval of 30−65-m to the Zhoukoudianian Stage; and the depth interval of 65−215-m to the Nihewanian Stage. The base of the interval of Quaternary deposition is located within the Yinggehai Formation.

#### *4.6.3 Continental shelf deposits in eastern China*

The chronostratigraphic frameworks of the continental shelf deposits in eastern China have been well established in the Bohai Sea and southern Yellow Sea, but less so in the northern Yellow Sea and the East China Sea (Yuan et al., 2014; Liu et al., 2015; Yi et al., 2016a, 2016bb; Xu et al., 2017, 2018). The Quaternary deposits around the Bohai Sea consist of two parts: an upper part comprising marine deposits associated with transgressions during the late Quaternary; and a lower part comprising fluvio-lacustrine deposits.

The late Quaternary deposits record three major transgressions around the Bohai Sea (Zhao et al., 1978), including from oldest to youngest, the Cangzhou transgression, the Huanghua transgression (Bohai transgression enclosed) and

the Xianxian transgression. The three transgressions have been constrained to MIS 7, MIS 5−3, and the Holocene, respectively, by integrating radiocarbon dating, luminescence dating, magnetostratigraphy and astronomical tuning (Yi et al., 2016a).

The fluvio-lacustrine deposits underlying the above-mentioned marine transgression deposits can be further subdivided into three parts: the lower part comprising fluvial and alluvial fine- to coarse-grained sands, the middle part comprising lacustrine clayey silts, and the upper part comprising lacustrine sediments intercalated with the sediments of several marine transgressions. Magnetostratigraphic studies (Yuan et al., 2014; Yi et al., 2016b; Xu et al., 2017, 2018) indicate that the onset of the fluvio-lacustrine deposits occurred during the terminal Miocene; they have variable thicknesses due to local faulting activity or to major changes in sedimentary environments. The M-B boundary is usually shallower than 150-m depth, and depths of the G-M boundary range from 476 m to 150 m.

Considering all the available chronostratigraphic evidence from around the Bohai Sea, the evolution of the Bohai continental shelf (or Bohai Bay Basin) since the Early Pliocene can be divided into three distinct phases with significant changes in depositional environments (Yi et al., 2016a, 2016b): (1) Phase I occurred prior to ~3.7 Ma and is characterized by rapid subsidence of Bohai Bay Basin with the dominance of alluvial and fluvial deposits belonging to the Gaozhuangian Stage. (2) Phase II occurred between ~3.7 Ma and ~0.3 Ma and is characterized by relatively slow subsidence of the basin, during which the Bohai paleolake developed and was isolated by the Miaodao Uplift. This phase is dominated by lacustrine deposits, which span the interval from the Mazegouan Stage, through the Nihewanian Stage, to the Zhoukoudianian Stage. (3) Phase III spans the interval from ~0.3 Ma to the present and is characterized by the termination of the Bohai paleolake due to the subsidence of the Miaodao Uplift. The phase is dominated by marine deposits, which belong to the Zhoukoudianian and Salawusuan Stages.

The Quaternary deposits in the Yellow Sea have a similar stratigraphy to those in the Bohai Sea, with the upper part consisting of marine deposits and the lower part of continental deposits. Long sedimentary sequences with magnetostratigraphic constraints mainly came from the southern Yellow Sea, including cores QC2 (Zhou and Ge, 1990), EY02-2 (Ge et al., 2006), NHH01 (Liu et al., 2014), DLC70-3 (Mei et al., 2016) and CSDP-1 (Liu et al., 2016a). The magnetostratigraphies of the cores show that the depths of the M-B boundary range from 60 m to 70 m. Moreover, the base of the Quaternary in the continental shelf of the Yellow Sea was first identified in core CSDP-1 by Liu et al. (2016a), at a depth of 227.16 m; the age of bottom of the core was estimated to be ~3.5 Ma (Liu et al., 2016a). Based on magnetostratigraphy and sedimentologic characteristics, Liu et al. (2016a) suggested that the transgression arrived at the drilling site of CSDP-1 no later than 1.7 Ma. They further suggested that the central part of the southern Yellow Sea has been dominated by marine deposits since ~1.0 Ma, while the western part has been dominated by marine sediments since ~0.7 Ma. In summary, in the southern Yellow Sea, the sedimentary sequences of the Nihewanian and Zhoukoudianian Stages are of continental and marine origin, respectively.

## 5. Stratigraphic framework of the Quaternary in China

The Quaternary strata in China are mainly of continental origin, with a nationwide distribution and consisting of a variety of deposit types. The continental Quaternary in northern China consists mainly of eolian and fluvio-lacustrine deposits; that in southern China, mainly of the red soil sequence (that is, vermiculated red soil), cave/fissure deposits, and fluvio-lacustrine deposits; and that in the alpine Tibetan Plateau, mainly of fluvio-lacustrine and piedmont deposits. The marine Quaternary is distributed in the Bohai Sea, Yellow Sea, East China Sea and South China Sea. Likewise, the marine Quaternary consists mainly of detrital deposits. Quaternary biogenic reef deposits are distributed only in the South China Sea.

In Cheng et al. (2009), the characteristics of tectonics, paleoclimate and paleogeography during the Quaternary enable China to be zoned into four regions: western China, central China, eastern China, and the marine area including islands (Zhou et al., 2000; Cheng et al., 2009).

In China, the paleogeographic, paleogeomorphologic and paleoenvironmental patterns during the Quaternary were similar to those of today. However, the characteristics of the biotas and deposit types are distinct between northern and southern China, with the boundary consisting of the Qinling Mountains and the Huaihe River. Hence, in the next section we describe the continental strata within China as being zoned into two regions, northern and southern China, and describe the marine strata without subdivision.

### 5.1 Continental Quaternary in northern China

The Quaternary in northern China consists mainly of eolian and fluvio-lacustrine deposits, and cave deposits have limited distributions in the Qinling Mountains, North China Plain and northeastern China. The eolian deposits are typified by the CLP loess-paleosol sequence. Within and around the plateau, there is a sporadic distribution of fluvio-lacustrine deposits and eolian dunes. Typical fluvio-lacustrine deposits are distributed in sedimentary basins outside the plateau, e.g., in the Songliao Basin, Nihewan Basin, San-

menxia Basin, and Weihe Basin.

In northern China, typical strata of the Nihewanian Stage include the Wucheng Loess and the lower part of the Lishi Loess (i.e., the loess-paleosol sequence from L33 to L8), the Nihewan Formation in the Nihewan Basin, the middle part of the Sanmen Formation (i.e., the lower to middle parts of the yellow Sanmen Formation, and the Haiyan and Louzeyu Formations in the Yushe Basin.

Typical strata of the Zhoukoudianian Stage include the upper part of the Lishi Loess (that is, the loess-paleosol sequence from L8 to L2), the Zhoukoudian Formation of Zhoukoudian Locality 1, the Xiaodukou Formation in the Nihewan Basin, and the upper part of the Sanmen Formation in the Sanmenxia Basin.

Typical strata of the Salawusuan Stage include the Malan Loess and the top of the Lishi Loess (i.e., the last glacial loess unit L1 and the last interglacial soil unit S1), the Salawusu and Chengchuan Formations in the drainage area of the Salawusu River, and the Xujiayao Formation in the Nihewan Basin.

The typical Holocene strata include black loam (i.e., the Holocene soil S0) and the Holocene loess (L0), lacustrine deposits, and cave stalagmites in some areas.

### 5.2 Continental Quaternary in southern China

In tropical and subtropical southern China, the warm and humid climatic conditions and extensive distribution of Paleozoic and Mesozoic carbonates led to the dominance of red soils and cave/fissure deposits during the Quaternary. Quaternary fluvio-lacustrine deposits are distributed only in some small basins. The loess-paleosol sequence of eolian origin is developed in the lower reaches of the Yangtze River, which is also named the Xiashu Loess. Within the Tibetan Plateau, Quaternary deposits consist mainly of scattered fluvio-lacustrine sediments. In the surrounding regions of the Tibetan Plateau, Quaternary piedmont deposits are usually well developed, consisting of alluvial and proluvial fan sediments usually bearing gravels. In addition, a Quaternary loess-paleosol sequence of eolian origin is well developed in the eastern margin of the Tibetan Plateau, western Sichuan Province.

In southern China, the representative strata of the Nihewanian Stage include the lower part of the red soil sequence (that is, the vermiculated red soil); the cave deposits in the Chongzuo area and the Bubing Basin (Guangxi) bearing the *Gigantopithecus-Sinomastodon* fauna, the cave deposits in the Longgupo of Wushan area (Chongqing City), the middle-lower parts of the borehole sedimentary sequence (152.00−614.47 m in depth) in the Heqing Basin (Yunnan), the Yuanmou Formation and the upper part of the Shagou Formation in the Yuanmou Basin (Yunnan), and the fluvial and alluvial sediments in the upper part of the Sanying Formation in the Dali Basin (Yunnan) with a thickness of ~215 m, and fluvio-lacustrine and alluvial sediments in the upper part of the Zanda Formation in the Zanda Basin (Tibet) with a thickness of ~180 m.

The representative strata of the Zhoukoudianian Stage include the upper part of the red soil sequence, the cave deposits bearing the *Ailuropoda-Stegodon* fauna, the upper part of the borehole sedimentary sequence in the Heqing Basin, the lower-middle parts of the Xiashu Loess, and cave stalagmites (e.g., Sanbao and Dongge Caves).

The representative strata of the Salawusuan Stage include the upper part of Xiashu Loess, the uppermost part of the borehole sedimentary sequence in the Heqing Basin, cave stalagmites, and several cave clastic deposits bearing human fossils.

The typical Holocene strata include the uppermost part of the Xiashu Loess, lacustrine sediments, and cave stalagmites.

In addition, the eolian deposits in western Sichuan Province comprise a loess-paleosol sequence of the upper part of the Mazegouan Stage (Upper Pliocene), the Nihewanian Stage (Lower Pleistocene), the Zhoukoudianian Stage (Middle Pleistocene) and the Salawusuan Stage (Upper Pleistocene).

### 5.3 Marine Quaternary

Quaternary marine strata are widely distributed in the Bohai Sea, the Yellow Sea, the East China Sea and the South China Sea, which are dominated by detrital deposits. Biogenic reefs are only developed in the South China Sea.

In the continental shelves of eastern China, Quaternary chronostratigraphic frameworks have been well established in the Bohai Sea and the southern Yellow Sea. In the Bohai Sea and its surrounding regions, marine deposits have been developed since ~0.3 Ma; and in the southern Yellow Sea, since ~1.0 Ma in the middle part, and since ~0.7 Ma in the western part.

In the South China Sea, Quaternary chronostratigraphic frameworks have been well established, including those of the detrital sedimentary sequence of ODP Leg 184 and the biogenic reef sequence of the Xike-1 borehole.

The representative strata of the Nihewanian Stage include the middle-lower parts of the Ledong Formation and the upper part of the Yinggehai Formation of the Xike-1 borehole, and the sedimentary sequence with an age interval of MIS 103−19 in the sites of ODP Leg 184.

The representative strata of the Zhoukoudianian Stage include the upper 60−70 m detrital sedimentary sequence in the southern Yellow Sea, the upper 30−65 m biogenic reef sequence in the Xike-1 borehole, and the detrital sedimentary sequence with an age interval of MIS 19−5 in the sites of ODP Leg 184.

The representative strata of the Salawusuan Stage include

the upper 30 m biogenic reef sequence in the Xike-1 borehole, and the detrital sedimentary sequence with an age interval of MIS 5−2 in the sites of ODP Leg 184.

Holocene marine deposits are extensively distributed in the Bohai Sea, the Yellow Sea, the East China Sea and the South China Sea.

## 6. Summary and future directions

The Quaternary strata in China mainly comprise continental deposits. For Quaternary marine strata, the high-precision climatochronostratigraphy based on oxygen isotope stages has been well established, as represented by that of ODP Leg 184 sites in the South China Sea. Therefore, the summary and future directions described below focus on Quaternary continental strata.

Chronostratigraphic frameworks of Quaternary continental strata on the scales of Quaternary geomagnetic polarities have been established by combining magnetic stratigraphy and biostratigraphy, which have effectively facilitated regional stratigraphic correlation among sedimentary basins and deposit types. High-precision chronostratigraphy of continental Quaternary has culminated in the chronology of the CLP loess-paleosol sequence, which has been achieved by establishing correlations between paleoclimatic proxies (e.g., magnetic susceptibility, grain size) and marine oxygen isotope records, and further by orbital tuning of the paleoclimatic proxies. The resulting high-precision timescales of Chinese loess have enabled orbital-scale stratigraphic correlation among loess sections.

A standard geologic time scale is the fundamental tool in geoscience. The establishment of precise and accurate chronostratigraphic charts is valuable not only for theoretical research but also for applied fields such as natural resources, environments and engineering. The Mesozoic-Cenozoic strata in China, especially in eastern China, are mainly of continental origin. Therefore, both continental stratigraphic correlation and marine-continental correlation should be considered when establishing Mesozoic-Cenozoic chronostratigraphic charts in China. Specifically, the chronostratigraphy of the Chinese continental Quaternary is characterized by the close integration of magnetostratigraphy and climatostratigraphy. Several aspects of future research in establishing the Chinese Quaternary chronostratigraphic chart are suggested below.

Biostratigraphy has provided a basic reference for Quaternary chronostratigraphy, and more detailed Quarternary biostratigraphic investigations should be conducted. The first effort should be a climatochronostratigraphic sequence of representative faunas by incorporating the well-constrained chronologies based on multiple dating methods with paleoenvironmental reconstructions based on multiple proxies, which enables the effective integration of biochronostratigraphy and climatochronostratigraphy.

Age determinations based on radiometric isotopic methods cannot be satisfactorily applied to the Chinese continental Quaternary due to the absence of required materials (e.g., tuff layers). Therefore, a secondary effort is to establish high-precision timescales for representative non-eolian sedimentary sequences by incorporating magnetic stratigraphy with orbital tuning, which facilitates orbital-scale stratigraphic correlation between the non-eolian sequences of different deposit types and the CLP loess-paleosol sequence, and further enables orbital-scale stratigraphic correlation among different regions and depositional settings.

The final effort is to incorporate the above-mentioned high-precision climatochronostratigraphy of the continental Quaternary with previously published high-precision climatochronostratigraphy of the marine Quaternary, thus enabling precise stratigraphic correlation of glacial-interglacial cycles between continental and marine Quaternary strata. Ultimately, those efforts will lead to the establishment not only of a Chinese continental Quaternary climatochronostratigraphic chart on the scale of glacial-interglacial cycles but also of a Quaternary integrative chronostratigraphic chart involving both continental and marine strata in China.

**Acknowledgements** *We are grateful to Profs. Jiayu Rong and Shuzhong Shen for their suggestion to write this review; to Prof. Shuzhong Shen, Dr. Junyi Ge, and the two anonymous reviewers for helpful comments and suggestions for improving the manuscript; to Dr. Lu Sun for help with drafting figures; and to Dr. Jan Bloemendal for improving the English. Chenglong Deng thanks Lu Sun, Liang Yi, Caicai Liu, Shihu Li, Shuhui Cai, Jianxing Liu, Qinmian Xu, Shixia Yang, Ping Liu, Yan Zhang and Suzhen Liu for useful discussion. This study was supported by the National Natural Science Foundation of China (Grant Nos. 41690110, 41621004 and L152401).*

## References

Aguirre E, Pasini G. 1985. The Pliocene-Pleistocene boundary. Episodes, 8: 116−120

An Z S, Clemens S C, Shen J, Qiang X K, Jin Z D, Sun Y B, Prell W L, Luo J J, Wang S M, Xu H. 2011. Glacial-interglacial Indian summer monsoon dynamics. Science, 333: 719−723

An Z S, Ho C K. 1989. New magnetostratigraphic dates of Lantian *Homo erectus*. Quat Res, 32: 213–221

Bae C J, Wang W, Zhao J, Huang S, Tian F, Shen G. 2014. Modern human teeth from Late Pleistocene Luna Cave (Guangxi, China). Quat Int, 354: 169–183

Barbour G B. 1924. Preliminary observations in the Kalgan Area. Bull Geol Soc China, 3: 153−168

Bien M N. 1940. Preliminary observation on the Cenozoic geology of Yunnan. Bull Geol Soc China, 20: 179−194

Black D, Teilhard de Chardin P, Young C C, Pei W C. 1933. Fossil Man in China: The Choukoutien cave deposits with a synopsis of our present knowledge of the Late Cenozoic in China. Mem Geol Survey China (Ser A), 11: 1−174

Chen T M, Yuan S X, Gao S J, Wang L X, Zhao G Y. 1982. Dating of the Peking Man site: Uranium series dating of the Xujiayao (Hsü-Chia-Yao) site (in Chinese). Acta Anthropol Sin, 1: 91−95

Chen T M, Zhou L P. 2009. Dating of the Peking Man site: A comparison

between existing chronology and the $^{26}Al/^{10}Be$ burial ages (in Chinese). Acta Anthropol Sin, 28: 285−291
Cheng H, Edwards R L, Broecker W S, Denton G H, Kong X, Wang Y, Zhang R, Wang X. 2009. Ice age terminations. Science, 326: 248–252
Cheng H, Lawrence Edwards R, Shen C C, Polyak V J, Asmerom Y, Woodhead J, Hellstrom J, Wang Y, Kong X, Spötl C, Wang X, Calvin Alexander Jr. E. 2013. Improvements in $^{230}Th$ dating, $^{230}Th$ and $^{234}U$ half-life values, and U-Th isotopic measurements by multi-collector inductively coupled plasma mass spectrometry. Earth Planet Sci Lett, 371-372: 82–91
Cheng H, Edwards R L, Sinha A, Spötl C, Yi L, Chen S, Kelly M, Kathayat G, Wang X, Li X, Kong X, Wang Y, Ning Y, Zhang H. 2016. The Asian monsoon over the past 640000 years and ice age terminations. Nature, 534: 640–646
Cheng Y Q, Wang Z J, Huang Z G. 2009. Stratigraphical Lexicon of China (in Chinese). Beijing: Geological Publishing House. 1−411
Chesner C A, Rose W I. 1991. Stratigraphy of the Toba Tuffs and the evolution of the Toba Caldera Complex, Sumatra, Indonesia. Bull Volcanol, 53: 343–356
Chou M C. 1957. Characteristic and correlation of the Tertiary and early Quaternary mammalian faunas from southern China (in Chinese). Chin Sci Bull, 8: 394−400
Chou M C. 1961. Occurrence of Enhydriodon at Yuanmo, Yunnan (in Chinese). Verteb PalAsia, 5: 164−167
Ciochon R, Long V T, Larick R, Gonzalez L, Grun R, de Vos J, Yonge C, Taylor L, Yoshida H, Reagan M. 1996. Dated co-occurrence of *Homo erectus* and *Gigantopithecus* from Tham Khuyen Cave, Vietnam. Proc Natl Acad Sci USA, 93: 3016–3020
Deng C. 2008. Paleomagnetic and mineral magnetic investigation of the Baicaoyuan loess-paleosol sequence of the western Chinese Loess Plateau over the last glacial-interglacial cycle and its geological implications. Geochem Geophys Geosyst, 9: Q04034
Deng C, Liu Q, Wang W, Liu C. 2007. Chemical overprint on the natural remanent magnetization of a subtropical red soil sequence in the Bose Basin, southern China. Geophys Res Lett, 34: L22308
Deng C, Xie F, Liu C, Ao H, Pan Y, Zhu R. 2007. Magnetochronology of the Feiliang Paleolithic site in the Nihewan Basin and implications for early human adaptability to high northern latitudes in East Asia. Geophys Res Lett, 34: L14301
Deng C, Shaw J, Liu Q, Pan Y, Zhu R. 2006a. Mineral magnetic variation of the Jingbian loess/paleosol sequence in the northern Loess Plateau of China: Implications for Quaternary development of Asian aridification and cooling. Earth Planet Sci Lett, 241: 248–259
Deng C, Wei Q, Zhu R, Wang H, Zhang R, Ao H, Chang L, Pan Y. 2006b. Magnetostratigraphic age of the Xiantai Paleolithic site in the Nihewan Basin and implications for early human colonization of Northeast Asia. Earth Planet Sci Lett, 244: 336–348
Deng C, Zhu R, Zhang R, Ao H, Pan Y. 2008. Timing of the Nihewan formation and faunas. Quat Res, 69: 77–90
Deng T. 2006. Chinese Neogene mammal biochronology (in Chinese). Verteb PalAsia, 44: 143−163
Deng T, Xue X X. 1997. Redemonstrating the first appearance of the genus *Equus* as a sign of the lower boundary of the Quaternary (in Chinese). J Stratigr, 21: 109−116
Deng T, Hou S K. 2011. The Mazegouan Stage of the continental Pliocene Series in China (in Chinese). J Stratigr, 35: 237−249
Deng T, Hou S K, Wang T M, Mu Y Q. 2010. The Gaozhuangian Stage of the continental Pliocene Series in China (in Chinese). J Stratigr, 34: 225−240
Ding Z L, Derbyshire E, Yang S L, Yu Z W, Xiong S F, Liu T S. 2002. Stacked 2.6-Ma grain size record from the Chinese loess based on five sections and correlation with the deep-sea $\delta^{18}O$ record. Paleoceanography, 17: 5-1–5-21
Ding Z L, Liu T S. 1989. Progresses of loess research in China (Part 1): Loess stratigraphy (in Chinese). Quat Sci, 9: 24−35
Ding Z L, Sun J M, Liu T S, Zhu R X, Yang S L, Guo B. 1998. Wind-blown origin of the Pliocene red clay formation in the central Loess Plateau, China. Earth Planet Sci Lett, 161: 135–143
Ding Z, Yu Z, Rutter N W, Liu T. 1994. Towards an orbital time scale for chinese loess deposits. Quat Sci Rev, 13: 39–70
Editorial Board of Chinese Geology, Institute of Geology of Academia Sinica. 1956. Chinese Regional Stratigraphic Chart (Draft) (in Chinese). Beijing: Science Press. 693
Edwards R, Chen J H, Wasserburg G J. 1987. $^{238}U$-$^{234}U$-$^{230}Th$-$^{232}Th$ systematics and the precise measurement of time over the past 500,000 years. Earth Planet Sci Lett, 81: 175–192
Fang X. 2002. Loess in Kunlun Mountains and its implications on desert development and Tibetan Plateau uplift in west China. Sci China Ser D: Earth Sci, 45: 289–299
Fu C, An Z, Qiang X, Bloemendal J, Song Y, Chang H. 2013. Magnetostratigraphic determination of the age of ancient Lake Qinghai, and record of the East Asian monsoon since 4.63 Ma. Geology, 41: 875–878
Ge J, Guo Z, Zhan T, Yao Z, Deng C, Oldfield F. 2012. Magnetostratigraphy of the Xihe loess-soil sequence and implication for late Neogene deformation of the West Qinling Mountains. Geophys J Int, 189: 1399–1408
Ge S L, Shi X F, Zhu R X, Liu Y G, Yin P, Liu L J. 2006. Magnetostratigraphy of borehole EY02-2 in the southern Yellow Sea and its paleoenvironmental significance. Chin Sci Bull, 51: 855−865
Gibbard P L, Head M J, Walker M J C. 2010. Formal ratification of the Quaternary System/Period and the Pleistocene Series/Epoch with a base at 2.58 Ma. J Quat Sci, 25: 96–102
Gradstein F M, Ogg J G, Smith A G. 2004. A Geologic Time Scale 2004. Cambridge: Cambridge University Press. 589
Gradstein F M, Ogg J G, Schmitz M D, Ogg G M. 2012. The Geologic Time Scale 2012. Amsterdam: Elsevier. 1144
Guo Z T. 2017. Loess Plateau attests to the onsets of monsoon and deserts (in Chinese). Sci Sin Terrae, 47: 421−437
Guo Z, Biscaye P, Wei L, Chen X, Peng S, Liu T. 2000. Summer monsoon variations over the last 1.2 Ma from the weathering of loess-soil sequences in China. Geophys Res Lett, 27: 1751–1754
Guo Z T, Ruddiman W F, Hao Q Z, Wu H B, Qiao Y S, Zhu R X, Peng S Z, Wei J J, Yuan B Y, Liu T S. 2002. Onset of Asian desertification by 22 Myr ago inferred from loess deposits in China. Nature, 416: 159–163
Han F, Bahain J J, Deng C, Boëda É, Hou Y, Wei G, Huang W, Garcia T, Shao Q, He C, Falguères C, Voinchet P, Yin G. 2017. The earliest evidence of hominid settlement in China: Combined electron spin resonance and uranium series (ESR/U-series) dating of mammalian fossil teeth from Longgupo cave. Quat Int, 434: 75–83
Hao Q, Guo Z. 2004. Magnetostratigraphy of a late Miocene-Pliocene loess-soil sequence in the western Loess Plateau in China. Geophys Res Lett, 31: L09209
Hao Q, Guo Z, Qiao Y, Xu B, Oldfield F. 2010. Geochemical evidence for the provenance of middle Pleistocene loess deposits in southern China. Quat Sci Rev, 29: 3317–3326
Hao Q, Wang L, Oldfield F, Peng S, Qin L, Song Y, Xu B, Qiao Y, Bloemendal J, Guo Z. 2012. Delayed build-up of Arctic ice sheets during 400,000-year minima in insolation variability. Nature, 490: 393–396
Heller F, Tung-sheng L. 1982. Magnetostratigraphical dating of loess deposits in China. Nature, 300: 431–433
Heller F, Tungsheng L. 1984. Magnetism of Chinese loess deposits. Geophys J Int, 77: 125–141
Heller F, Tung-sheng L. 1986. Palaeoclimatic and sedimentary history from magnetic susceptibility of loess in China. Geophys Res Lett, 13: 1169–1172
Heslop D, Langereis C G, Dekkers M J. 2000. A new astronomical timescale for the loess deposits of Northern China. Earth Planet Sci Lett, 184: 125–139
Hilgen F J, Lourens L J, Van Dam J A. 2012. The Neogene Period. In: Gradstein F M, Ogg J G, Schmitz M D, Ogg G M, eds. The Geologic Time Scale 2012, Vol. 2. Amsterdam: Elsevier. 923–978
Hou L H. 1985. Fossil birds from Zhoukoudian Loc. 1. In: Wu R K et al. Multi-disciplinary Study of the Peking Man Site at Zhoukoudian (in

Chinese). Beijing: Science Press. 113–118
Hou Y M, Potts R, Yuan B, Guo Z T, Deino A, Wang W, Clark J, Xie G, Huang W W. 2000. Mid-Pleistocene Acheulean-like stone technology of the Bose Basin, South China. Science, 287: 1622−1626
Hovan S A, Rea D K, Pisias N G, Shackleton N J. 1989. A direct link between the China loess and marine $\delta^{18}$O records: Aeolian flux to the north Pacific. Nature, 340: 296–298
Hu C K. 1985. The history of mammalian fauna of Locality 1 of Zhoukoudian and its recent advances. In: Wu R K, ed. Multi-disciplinary Study of the Peking Man Site at Zhoukoudian (in Chinese). Beijing: Science Press. 107–113
Huang L. 1997. Calcareous nannofossil biostratigraphy in the Pearl River Mouth Basin, South China Sea, and Neogene reticulofenestrid coccoliths size distribution pattern. Mar Micropaleont, 32: 31–57
Jiang F C, Wu X H, Xiao H G, Zhao Z Z, Wang S M, Xue B. 1997. Age of the vermiculated red soil in Jiujiang area, central China (in Chinese). J Geomech, 3: 27−32
Jin C Z, Qin D G, Pan W S, Tang Z L, Liu J Y, Wang Y, Deng C L, Zhang Y Q, Dong W, Tong H W. 2009. A newly discovered *Gigantopithecus* fauna from Sanhe Cave, Chongzuo, Guangxi, South China. Chin Sci Bull, 54: 788−797
Jin C, Wang Y, Deng C, Harrison T, Qin D, Pan W, Zhang Y, Zhu M, Yan Y. 2014. Chronological sequence of the early Pleistocene *Gigantopithecus* faunas from cave sites in the Chongzuo, Zuojiang River area, South China. Quat Int, 354: 4–14
Jin C Z, Zheng J J, Wang Y, Xu Q Q. 2008. The stratigraphic distribution and zoogeography of the Early Pleistocene mammalian fauna from South China (in Chinese). Acta Anthropol Sin, 27: 304−317
Kong L J, Shen G J, Wang W, Li D W, Zhao J X. 2012. U-series dating of Shizi Cave and age of the third terrace of the Bubing and Baise Basins, Guangxi, China (in Chinese). Earth and Environ, 40: 349–353
Kong P, Jia J, Zheng Y. 2013. Cosmogenic $^{26}$Al/$^{10}$Be burial dating of the Paleolithic at Xihoudu, North China. J Human Evol, 64: 466–470
Kukla G, Heller F, Ming L X, Chun X T, Sheng L T, Sheng A Z. 1988. Pleistocene climates in China dated by magnetic susceptibility. Geology, 16: 811–814
Li B S, Jin H L, Zhu Y Z, Dong G R, Wen X H. 2004a. The Quaternary lithostrata in Salawusu River Valley and their geochronology (in Chinese). Acta Sediment Sin, 22: 676−682
Li X, Zhao Q H, Huang B Q, Su X. 2004b. High-resolution age estimation of the Mid-Pleistocene impact event. Mar Geol Quat Geol, 24: 73−77
Li X Q, Li C S, Lu H Y, Dodson J R, Wang Y F. 2004c. Paleovegetation and paleoclimate in middle-late Pliocene, Shanxi, central China. Palaeogeogr Palaeoclimatol Palaeoecol, 210: 57–66
Li C K, Wu W Y, Qiu Z D. 1984. Chinese Neogene: subdivision and correlation (in Chinese). Verteb PalAsia, 22: 163−178
Li P, Qian F, Ma X, Pu Q, Xing L, Ju S. 1976. Preliminary study on the age of the Yuanmou Man by paleomagnetic technique (in Chinese). Sci China, 6: 579−591
Li S, Deng C, Yao H, Huang S, Liu C, He H, Pan Y, Zhu R. 2013. Magnetostratigraphy of the Dali Basin in Yunnan and implications for late Neogene rotation of the southeast margin of the Tibetan Plateau. J Geophys Res Solid Earth, 118: 791–807
Li X S, Han Z Y, Lu H Y, Chen Y, Li Y, Yuan X K, Zhou Y W, Jiang M Y, Lv C J. 2018. Onset of Xiashu loess deposition in southern China by 0.9 Ma and its implications for regional aridification. Sci China Earth Sci, 61: 256–269
Liang X R, Wei G J, Shao L, Li X H, Wang R C. 2001. Records of Toba eruptions in the South China Sea—Chemical characteristics of the glass shards from ODP 1143A. Sci China Ser D-Earth Sci, 44: 871−878
Liu C, Zhu X Y, Ye S J. 1977. A palaeomagnetic study on the cave-deposits of Zhoukoudian (Choukoutian), the locality of Sinanthropus (in Chinese). Sci Geol Sin, 12: 26−33
Liu C C, Deng C L, Liu Q S, Zheng L T, Wang W, Xu X M, Huang S, Yuan B Y. 2010a. Mineral magnetism to probe into the nature of palaeomagnetic signals of subtropical red soil sequences in southern China. Geophys J Int, 181: 1395−1410
Liu L J, Xu H Z, Cui Q P, Wang J. 2010b. Study on Quaternary stratigraphic division on Hebei Plain (in Chinese). Geogr Geo-Inf Sci, 26: 54−57
Liu C, Xu X, Yuan B, Deng C. 2008. Magnetostratigraphy of the Qiliting section (SE China) and its implication for geochronology of the red soil sequences in southern China. Geophys J Int, 174: 107–117
Liu J, Liu Q, Zhang X, Liu J, Wu Z, Mei X, Shi X, Zhao Q. 2016a. Magnetostratigraphy of a long Quaternary sediment core in the South Yellow Sea. Quat Sci Rev, 144: 1–15
Liu P, Wu Z, Deng C, Tong H, Qin H, Li S, Yuan B, Zhu R. 2016b. Magnetostratigraphic dating of the Shanshenmiaozui mammalian fauna in the Nihewan Basin, North China. Quat Int, 400: 202–211
Liu J X, Liu Q S, Shi X F, Wang C J, Chen J J. 2015. Progress of Quaternary chronological research in the Yellow Sea (in Chinese). Mar Geol Front, 31: 17−25
Liu J, Shi X, Liu Q, Ge S, Liu Y, Yao Z, Zhao Q, Jin C, Jiang Z, Liu S, Qiao S, Li X, Li C, Wang C. 2014. Magnetostratigraphy of a greigite-bearing core from the South Yellow Sea: Implications for remagnetization and sedimentation. J Geophys Res Solid Earth, 119: 7425–7441
Liu P, Deng C, Li S, Cai S, Cheng H, Baoyin Y, Wei Q, Zhu R. 2012. Magnetostratigraphic dating of the Xiashagou Fauna and implication for sequencing the mammalian faunas in the Nihewan Basin, North China. Palaeogeogr Palaeoclimatol Palaeoecol, 315-316: 75–85
Liu T S. 1985. Loess and the Environment. Beijing: China Ocean Press. 251
Liu T S, Shi Y F, Wang R J, Zhao Q H, Jian Z M, Cheng X R, Wang P X, Wang S M, Yuan B Y, Wu X Z, Qiu Z X, Xu Q Q, Huang W B, Huang W W, An Z S, Lu H Y. 2000. Table of Chinese Quaternary stratigraphic correlation remarked with climate change (in Chinese). Quat Sci, 20: 108−128
Liu T S, Zhang Z H. 1962. Loess in China (in Chinese). Acta Geol Sin, 42: 1−14
Liu X, Shen G, Tu H, Lu C, Granger D E. 2015. Initial $^{26}$Al/$^{10}$Be burial dating of the hominin site Bailong Cave in Hubei Province, central China. Quat Int, 389: 235–240
Lu H, Liu X, Zhang F, An Z, Dodson J. 1999. Astronomical calibration of loess-paleosol deposits at Luochuan, central Chinese Loess Plateau. Palaeogeogr Palaeoclimatol Palaeoecol, 154: 237–246
Lu H, Zhang H, Wang S, Cosgrove R, Sun X, Zhao J, Sun D, Zhao C, Shen C, Wei M. 2011. Multiphase timing of hominin occupations and the paleoenvironment in Luonan Basin, Central China. Quat Res, 76: 142–147
Lu H Y, Zhang H Y, Wang S J, Cosgrove R, Zhao C F, Stevens T, Zhao J. 2007. A preliminary survey on loess deposit in eastern Qinling Mountains (central China) and its implication for estimating age of the Pleistocene lithic artifacts (in Chinese). Quat Sci, 27: 559−567
Luo X, Rehkämper M, Lee D C, Halliday A N. 1997. High precision $^{230}$Th/$^{232}$Th and $^{234}$U/$^{238}$U measurements using energy-filtered ICP magnetic sector multiple collector mass spectrometry. Int J Mass Spectrometry Ion Processes, 171: 105–117
Mark D F, Renne P R, Dymock R C, Smith V C, Simon J I, Morgan L E, Staff R A, Ellis B S, Pearce N J G. 2017. High-precision $^{40}$Ar/$^{39}$Ar dating of pleistocene tuffs and temporal anchoring of the Matuyama-Brunhes boundary. Quat Geochron, 39: 1–23
Mei X, Li R, Zhang X, Liu Q, Liu J, Wang Z, Lan X, Liu J, Sun R. 2016. Evolution of the Yellow Sea warm current and the Yellow Sea cold water mass since the Middle Pleistocene. Palaeogeogr Palaeoclimatol Palaeoecol, 442: 48–60
Min L R, Zhu G X, Guan Y Y. 2009. An analysis of the basic characteristics of the Upper Pleistocene Salawusuan Stage in the Salawusu River Valley, Inner Mongolia (in Chinese). Geol China, 36: 1208−1217
National Commission on the Stratigraphy of China. 2017. Stratigraphical Guide of China and Its Explanation (in Chinese). Beijing: Geological Publishing House. 1−61
Nian X M, Zhou L P, Yuan B Y. 2013. Optically stimulated luminescence dating of terrestrial sediments in the Nihewan Basin and its implication

for the evolution of ancient Nihewan lake (in Chinese). Quat Sci, 33: 403−414
Pan Y X, Zhu R X, Liu Q S, Guo B, Yue L P, Wu H N. 2002. Geomagnetic episodes of the last 1.2 Myr recorded in Chinese loess. Geophys Res Lett, 29: 123-1–123-4
Pei W C. 1957. The zoogeographical divisions of Quaternary mammalian faunas of China. Verteb PalAsia, 1: 9−24
Pei W C. 1961. Fossil mammals of early Pleistocene age from Yuanmo (Ma-kai) of Yunnan (in Chinese). Verteb PalAsia, 5: 16−30
Pei W C, Chou M C, Zheng J J. 1963. Cenozoic Erathem of China (in Chinese). In: National Commission on Stratigraphy of China, ed. Selected Scientific Reports at All-China Stratigraphic Congress. Beijing: Science Press. 1−31
Pei W C, Huang W B. 1959. Some perspectives on the Sanmen Group (in Chinese). In: Chinese Association for Quaternary Research, ed. Proceedings of the Conference on Quaternary Geology of the Sanmenxia Basin. Beijing: Scicence Press. 3−20
Pillans B, Gibbard P. 2012. The Quaternary Period. In: Gradstein F M, Ogg J G, Schmitz M D, Ogg G M, eds. The Geologic Time Scale 2012. Vol. 2. Amsterdam: Elsevier. 979–1010
Pu Q Y, Qian F. 1977. Study on the fossil human strata—the Yuanmo Formation (in Chinese). Acta Geol Sin, 51: 89−100
Qian F. 1999. Study on magnetostratigraphy in Qinghai-Tibetan Plateau in late Cenozoic (in Chinese). J Geomech, 5: 22–34
Qian F, Zhou G X. 1991. Quaternary Geology and Paleoanthropology of Yuanmou, Yunnan, China (in Chinese). Beijing: Science Press. 222
Qian F, Zhang J X, Yin W D. 1985. Magnetic stratigraphy from the sediment of west wall and test pit of Locality 1 at Zhoukoudian (in Chinese). In: Wu R K, ed. Multi-disciplinary Study of the Peking Man Site at Zhoukoudian. Beijing: Science Press. 251−255
Qiang X K, Xu X W, Chen T, Zhao H, Zheng H T. 2016. Spatial characteristics and influence factors of Matuyama-Brunhes polarity reversal boundary (MBB) in eolian sequences from the Chinese Loess Plateau (in Chinese). Quat Sci, 36: 1125−1138
Qiao Y. 2003. Loess-soil sequences in southern Anhui Province: Magnetostratigraphy and paleoclimatic significance. Chin Sci Bull, 48: 2088–2093
Qiao Y S, Liu D Y, Li C Z, Li M Z, Wang Y, Zhao Z Z. 2007. Magnetostratigraphy of a loess-soil sequence in the Garze area, western Sichuan (in Chinese). J Geomech, 13: 289−296
Qiao Y S, Wang Y, Yao H T, Qi L, He Z X, Cheng Y, Peng S S, Ge J Y. 2015. Magnetostratigraphy of a loess-paleosol sequence from higher terrace of the Daduhe River in the eastern margin of the Tibetan Plateau and its geological significance. Acta Geol Sin, 89: 316–317
Qiu Z X. 2000. Nihewan fauna and Q/N boundary in China (in Chinese). Quat Sci, 20: 142−154
Qiu Z X, Huang W L, Guo Z H. 1987. The Chinese hipparioniae fossils (in Chinese). Paleontol Sin New Ser C, 25: 1−250
Qiu Z, Qiu Z. 1995. Chronological sequence and subdivision of Chinese Neogene mammalian faunas. Palaeogeogr Palaeoclimatol Palaeoecol, 116: 41–70
Rink W J, Wei W, Bekken D, Jones H L. 2008. Geochronology of *Ailuropoda-Stegodon* fauna and *Gigantopithecus* in Guangxi Province, southern China. Quat Res, 69: 377–387
Rio D, Sprovieri R, Castradori D, Di Stefano E. 1998. The Gelasian Stage (Upper Pliocene): A new unit of the global chronostratigraphic scale. Episodes, 21: 82–87
Saylor J E, Quade J, Dettman D L, DeCelles P G, Kapp P A, Ding L. 2009. The late Miocene through present paleoelevation history of southwestern Tibet. Am J Sci, 309: 1–42
Shao L, Zhu W L, Deng C L, Zhang Y C, Zhai S K. 2016. Reservoir Stratum Sedimentology of Carbonate Biogenic Reefs in Well Xike-1 From Xisha Islands, South China Sea: Chronostratigraphy and Paleoceanographic Environments (in Chinese). Wuhan: China University of Geosciences Press. 128
Shao Q, Wang W, Deng C, Voinchet P, Lin M, Zazzo A, Douville E, Dolo J M, Falguères C, Bahain J J. 2014. ESR, U-series and paleomagnetic dating of Gigantopithecus fauna from Chuifeng Cave, Guangxi, southern China. Quat Res, 82: 270–280
Shao Q, Wang Y, Voinchet P, Zhu M, Lin M, Rink W J, Jin C, Bahain J J. 2017. U-series and ESR/U-series dating of the *Stegodon-Ailuropoda* fauna at Black Cave, Guangxi, southern China with implications for the timing of the extinction of *Gigantopithecus blacki*. Quaternary Int, 434: 65–74
Shen C C, Lawrence Edwards R, Cheng H, Dorale J A, Thomas R B, Bradley Moran S, Weinstein S E, Edmonds H N. 2002. Uranium and thorium isotopic and concentration measurements by magnetic sector inductively coupled plasma mass spectrometry. Chem Geol, 185: 165–178
Shen G, Gao X, Gao B, Granger D E. 2009. Age of Zhoukoudian *Homo erectus* determined with $^{26}Al/^{10}Be$ burial dating. Nature, 458: 198–200
Shi N, Cao J X, Konigsson L K. 1993. Late Cenozoic vegetational history and the Pliocene-Pleistocene boundary in the Yushe Basin, S.E. Shanxi, China. Grana, 32: 260–271
Singer B S. 2014. A Quaternary geomagnetic instability time scale. Quat Geochron, 21: 29–52
Singer B S, Guillou H, Jicha B R, Zanella E, Camps P. 2014. Refining the Quaternary Geomagnetic Instability Time Scale (GITS): Lava flow recordings of the Blake and Post-Blake excursions. Quat Geochron, 21: 16–28
Stevens T, Armitage S J, Lu H, Thomas D S G. 2006. Sedimentation and diagenesis of Chinese loess: Implications for the preservation of continuous, high-resolution climate records. Geology, 34: 849–852
Sun D, Liu D, Chen M, An Z, John S. 1997. Magnetostratigraphy and palaeoclimate of Red Clay sequences from Chinese Loess Plateau. Sci China Ser D-Earth Sci, 40: 337–343
Sun L, Deng C, Wang W, Liu C, Kong Y, Wu B, Liu S, Ge J, Qin H, Zhu R. 2017a. Magnetostratigraphy of Plio–Pleistocene fossiliferous cave sediments in the Bubing Basin, southern China. Quat Geochronology, 37: 68–81
Sun X, Lu H, Wang S, Yi L, Li Y, Bahain J J, Voinchet P, Hu X, Zeng L, Zhang W, Zhuo H. 2017b. Early human settlements in the southern Qinling Mountains, central China. Quat Sci Rev, 164: 168–186
Sun L, Wang Y, Liu C, Zuo T, Ge J, Zhu M, Jin C, Deng C, Zhu R. 2014. Magnetochronological sequence of the Early Pleistocene *Gigantopithecus* faunas in Chongzuo, Guangxi, southern China. Quat Int, 354: 15–23
Sun Y, Clemens S C, An Z, Yu Z. 2006. Astronomical timescale and palaeoclimatic implication of stacked 3.6-Myr monsoon records from the Chinese Loess Plateau. Quat Sci Rev, 25: 33–48
Tedford R H, Flynn L J, Zhanxiang Q, Opdyke N D, Downs W R. 1991. Yushe Basin, China; Paleomagnetically calibrated mammalian biostratigraphic standard from the late Neogene of eastern Asia. J Vert Paleont, 11: 519–526
Tedford R H, Qiu Z X, Flynn L J. 2013. Late Cenozoic Yushe Basin, Shanxi Province, China: Geology and Fossil Mammals. Vol. I: History, Geology and Magnetostratigraphy. Dordrecht: Springer. 109
Teilhard de Chardin P, Licent E. 1924. On the Geology of the Northern, Western and Southern Borders of the Ordos, China. Bull Geol Soc China, 3: 37−44
Teilhard de Chardin P, Piveteau J. 1930. Les mammifères fossiles de Nihowan (Chine). Annales de Paléontologie, 19: 1−134
Tian J, Wang P, Cheng X, Li Q. 2002. Astronomically tuned Plio–Pleistocene benthic $\delta^{18}O$ record from South China Sea and Atlantic–Pacific comparison. Earth Planet Sci Lett, 203: 1015–1029
Tong G B, Shi Y, Zheng H R, Zhang J, Lin F, He Q L, Song X H, Liu Z X, Qiao G D, Zhang J X, Yang X D, Zhang W Q. 1998. Quaternary stratigraphy in Yinchuan Basin (in Chinese). J Stratigr, 22: 42−51
Tong H W, Li H, Xie J Y. 2008. Revisions of some taxa of the Salawusu Fauna from Sjara-Osso-Gol area, Neimongol, China (in Chinese). Quat Sci, 28: 1106−1113
Walker M, Johnsen S, Rasmussen S O, Steffensen J P, Popp T, Gibbard P, Hoek W, Lowe J, Andrews J, Bjorck S, Cwynar L, Hughen K, Kershaw P, Kromer B, Litt T, Lowe D J, Nakagawa T, Newnham R, Schwande J.

2008. The Global Stratotype Section and Point (GSSP) for the base of the Holocene Series/Epoch (Quaternary System/Period) in the NGRIP ice core. Episodes, 31: 264−267
Wang H. 1988. An early Pleistocene mammalian fauna from Dali, Shaanxi (in Chinese). Verteb PalAsia, 26: 59−72
Wang H, Deng C, Zhu R, Wei Q, Hou Y, Boëda E. 2005a. Magnetostratigraphic dating of the Donggutuo and Maliang Paleolithic sites in the Nihewan Basin, North China. Quat Res, 64: 1–11
Wang X, Løvlie R, Yang Z, Pei J, Zhao Z, Sun Z. 2005b. Remagnetization of Quaternary eolian deposits: A case study from SE Chinese Loess Plateau. Geochem Geophys Geosyst, 6: Q06H18
Wang P, Zhao Q, Jian Z, Cheng X, Huang W, Tian J, Wang J, Li Q, Li B, Su X. 2003. Thirty million year deep sea records in the South China Sea. Chin Sci Bull, 48: 2524–2535
Wang S F, Zhang W L, Fang X M, Dai S, Kempf O. 2008. Magnetostratigraphy of the Zanda basin in southwest Tibet Plateau and its tectonic implications. Chin Sci Bull, 53: 1393−1400
Wang S. 2002. Sedimentary records of environmental evolution in the Sanmen Lake Basin and the Yellow River running through the Sanmenxia Gorge eastward into the sea. Sci China Ser D: Earth Sci, 45: 595–608
Wang W, Potts R, Baoyin Y, Huang W, Cheng H, Edwards R L, Ditchfield P. 2007a. Sequence of mammalian fossils, including hominoid teeth, from the Bubing Basin caves, South China. J Human Evol, 52: 370–379
Wang X, Qiu Z, Li Q, Wang B, Qiu Z, Downs W R, Xie G, Xie J, Deng T, Takeuchi G T, Tseng Z J, Chang M, Liu J, Wang Y, Biasatti D, Sun Z, Fang X, Meng Q. 2007b. Vertebrate paleontology, biostratigraphy, geochronology, and paleoenvironment of Qaidam Basin in northern Tibetan Plateau. Palaeogeogr Palaeoclimatol Palaeoecol, 254: 363–385
Wang X M, Flynn L J, Fortelius M, eds. 2013a. Fossil Mammals of Asia: Neogene Biostratigraphy and Chronology. New York: Columbia University Press. 732
Wang X, Li Q, Xie G, Saylor J E, Tseng Z J, Takeuchi G T, Deng T, Wang Y, Hou S, Liu J, Zhang C, Wang N, Wu F. 2013b. Mio-Pleistocene Zanda Basin biostratigraphy and geochronology, pre-Ice Age fauna, and mammalian evolution in western Himalaya. Palaeogeogr Palaeoclimatol Palaeoecol, 374: 81–95
Wang X, Yang Z, Løvlie R, Min L. 2004. High-resolution magnetic stratigraphy of fluvio-lacustrine succession in the Nihewan Basin, China. Quat Sci Rev, 23: 1187–1198
Wang X, Yang Z, Løvlie R, Sun Z, Pei J. 2006. A magnetostratigraphic reassessment of correlation between Chinese loess and marine oxygen isotope records over the last 1.1Ma. Phys Earth Planet Inter, 159: 109–117
Wang X, Lu H, Zhang H, Wu J, Hou X, Fu Y, Geng J. 2018. Distribution, provenance, and onset of the Xiashu Loess in Southeast China with paleoclimatic implications. J Asian Earth Sci, 155: 180–187
Wang Y, Jin C Z, Deng C L, Wei G B, Yan Y L. 2012. The first Sinomastodon (Gomphotheriidae, Proboscidea) skull from the Quaternary in China. Chin Sci Bull, 57: 4726–4734
Wang Y, Jin C Z, Mead J I. 2014. New remains of *Sinomastodon yangziensis* (Proboscidea, Gomphotheriidae) from Sanhe karst Cave, with discussion on the evolution of Pleistocene Sinomastodon in South China. Quat Int, 339–340: 90–96
Wang Y, Jin C, Pan W, Qin D, Yan Y, Zhang Y, Liu J, Dong W, Deng C. 2017. The Early Pleistocene *Gigantopithecus-Sinomastodon* fauna from Juyuan karst cave in Boyue Mountain, Guangxi, South China. Quat Int, 434: 4–16
Wang Y J, Cheng H, Edwards R L, An Z S, Wu J Y, Shen C C, Dorale J A. 2001. A high-resolution absolute-dated Late Pleistocene monsoon record from Hulu Cave, China. Science, 294: 2345–2348
Wang Y, Cheng H, Edwards R L, Kong X, Shao X, Chen S, Wu J, Jiang X, Wang X, An Z. 2008. Millennial- and orbital-scale changes in the East Asian monsoon over the past 224,000 years. Nature, 451: 1090–1093
Wang Z F, Zhang D J, Liu X Y, You L, Luo W, Yi L, Tan L C, Zhu Y H, Qin H F, Cheng H, Li Z Q, Xie Q, Che Z W, Deng C L, Zhu R X. 2017. Magnetostratigraphy and $^{230}$Th dating of Pleistocene biogenic reefs in XK-1 borehole from Xisha Islands, South China Sea (in Chinese). Chin J Geophys, 60: 1027−1038
Wu C L, Zhu C, Lu H Y, Ma C M, Zhu G Y, Zheng C G, Xun X W. 2006. Magnetostratigraphical dating of the Xiashu Loess in Nanjing area and its paleoenvironmental interpretation (in Chinese). J Stratigr, 30: 116−123
Wu R K, Ren M E, Zhu X M, Yang Z G, Hu C K, Kong Z C, Xie Y Y. 1985. Multi-disciplinary Study of the Peking Man Site at Zhoukoudian (in Chinese). Beijing: Science Press. 267
Xu Q M, Yang J L, Hu Y Z, Yuan G B, Deng C L. 2018. Magnetostratigraphy of two deep boreholes in southwestern Bohai Bay: Tectonic implications and constraints on the ages of volcanic layers. Quat Geochronol, 43: 1−13
Xu Q, Yuan G, Yang J, Xin H, Yi L, Deng C. 2017. Plio-Pleistocene magnetostratigraphy of northern Bohai Bay and its implications for tectonic events since ca. 2.0 Ma. J Geo Dyn, 111: 1–14
Xue X X. 1981. An early Pleistocene mammalian fauna and its stratigraphy of the River You, Weinan, Shensi (in Chinese). Verteb PalAsia, 19: 35−44
Yang S, Ding Z. 2010. Drastic climatic shift at ~2.8Ma as recorded in eolian deposits of China and its implications for redefining the Pliocene-Pleistocene boundary. Quat Int, 219: 37–44
Yao Y P, Liu Y. 2010. An international debate on the status of the Quaternary as a formal chronostratigraphical unit and the final ratification of the Quaternary System/Period (in Chinese). Adv Earth Sci, 25: 775−781
Yi L, Deng C, Tian L, Xu X, Jiang X, Qiang X, Qin H, Ge J, Chen G, Su Q, Chen Y, Shi X, Xie Q, Yu H, Zhu R. 2016. Plio-Pleistocene evolution of Bohai Basin (East Asia): demise of Bohai Paleolake and transition to marine environment. Sci Rep, 6: 29403
Yi L, Jiang X Y, Tian L Z, Yu H J, Xu X Y, Shi X F, Qin H F, Deng C L. 2016b. Geochronological study on Plio-Pleistocene evolution of Bohai Basin (in Chinese). Quat Sci, 36: 1075−1087
Yin Q, Guo Z. 2006. Mid-pleistocene vermiculated red soils in southern China as an indication of unusually strengthened East Asian monsoon. Chin Sci Bull, 51: 213–220
Young C C. 1950. The Plio-Pleistocene boundary in China. Report on 18th International Geological Congress, London. 115−125
Yuan B Y, Zhu R X, Tian W L, Cui J X, Li R Q, Wang Q, Yan F H. 1996. Magnetostratigraphic dating on the Nihewan Formation (in Chinese). Sci China Ser D: Earth Sci, 26: 67−73
Yuan B Y, Xia Z K, Li B S, Qiao Y S, Gu Z Y, Zhang J F, Xu B, Huang W W, Zeng R S. 2008. Chronostratigraphy and stratigraphic divisions of red soil in southern China (in Chinese). Quat Sci, 28: 1−13
Yuan D, Cheng H, Edwards R L, Dykoski C A, Kelly M J, Zhang M, Qing J, Lin Y, Wang Y, Wu J, Dorale J A, An Z, Cai Y. 2004. Timing, duration, and transitions of the Last Interglacial Asian Monsoon. Science, 304: 575–578
Yuan F L, Du H J. 1984. Cenozoic Stratigraphy in China (in Chinese). Beijing: Geological Publishing House. 233–249
Yuan G B, Xu Q M, Wang Y, Yang J L, Qin Y F, Du D. 2014. Magnetostratigraphy and tectonics significance of BG10 borehole in northern coast of Bohai Bay (in Chinese). Acta Geol Sin, 88: 285–298
Yue L P, Wang Y, Zheng H B. 1994. Magnetostratigraphic date on the "Yangguo Fauna" (in Chinese). J Stratigr, 18: 203−206
Yue L P, Xue X X. 1996. The comparative study of magnetostratigraphy and biostratigraphy in Chinese loess area (in Chinese). Quat Sci, 16: 239−244
Zan J, Fang X, Zhang W, Yan M, Zhang T. 2016. Palaeoenvironmental and chronological constraints on the Early Pleistocene mammal fauna from loess deposits in the Linxia Basin, NE Tibetan Plateau. Quat Sci Rev, 148: 234–242
Zeng L, Lu H, Yi S, Li Y, Lv A, Zhang W, Xu Z, Wu H, Feng H, Cui M. 2016. New magnetostratigraphic and pedostratigraphic investigations of loess deposits in north-east China and their implications for regional environmental change during the Mid-Pleistocene climatic transition. J Quat Sci, 31: 20–32

Zeng L, Lu H Y, Yi S W Xu Z W, Qiu Z M, Yang Z Y, Li Y X. 2011. Magnetostratigraphy of loess in northeastern China and paleoclimatic changes (in Chinese). Chin Sci Bull, 56: 2267–2275
Zhang J F, Huang W W, Hu Y, Yang S X, Zhou L P. 2015. Optical dating of flowstone and silty carbonate-rich sediments from Panxian Dadong Cave, Guizhou, southwestern China. Quat Geochron, 30: 479–486
Zhang Y, Jin C, Cai Y, Kono R, Wang W, Wang Y, Zhu M, Yan Y. 2014. New 400–320 ka *Gigantopithecus blacki* remains from Hejiang Cave, Chongzuo City, Guangxi, South China. Quat Int, 354: 35–45
Zhang Z H, Liu P G, Qian F, Min L R, Wang Q, Zong G F. 1994. New development in research of late Cenozoic stratigraphy in Yuanmou Basin (in Chinese). Mar Geol Quat Geol, 14: 1−18
Zhang W, Yu L, Lu M, Zheng X, Ji J, Zhou L, Wang X. 2009. East Asian summer monsoon intensity inferred from iron oxide mineralogy in the Xiashu Loess in southern China. Quat Sci Rev, 28: 345–353
Zhao H, Lu Y, Wang C, Chen J, Liu J, Mao H. 2010. ReOSL dating of aeolian and fluvial sediments from Nihewan Basin, northern China and its environmental application. Quat Geochron, 5: 159–163
Zhao Q, Jian Z, Li B, Cheng X, Wang P. 1999. Microtektites in the Middle Pleistocene deep-sea sediments of the South China Sea. Sci China Ser D-Earth Sci, 42: 531–535
Zhao S L, Yang G F, Cang S X, Zhang H C, Huang Q F, Xia D X, Wang Y J, Liu F S, Liu C F. 1978. On the marine stratigraphy and coastlines of the western coast of the gulf of Bohai (in Chinese). Oceanol Limn Sin, 9: 15−25
Zhao Z Z, Qiao Y S, Wang Y, Fu J L, Wang S B, Li C Z, Yao H T, Jiang F C. 2007. Magnetostratigraphic and paleoclimatic studies on the Red Earth Formation from the Chengdu Plain in Sichuan Province, China. Sci China Ser D-Earth Sci, 50: 927–935
Zheng H B, Rolph T, Shaw J, An Z S. 1995. A detailed palaeomagnetic record for the last interglacial period. Earth Planet Sci Lett, 133: 339−351
Zhou L P, Shackleton N J. 1999. Misleading positions of geomagnetic reversal boundaries in Eurasian loess and implications for correlation between continental and marine sedimentary sequences. Earth Planet Sci Lett, 168: 117–130
Zhou M L, Min L R, Wang S F. 2000. China's Quaternary Stratigraphy (in Chinese). Beijing: Geological Publishing House. 1−122
Zhou M Q, Ge Z S. 1990. Magnetostratigraphic study of loose sediments in southern Yellow Sea and its adjacent land area (in Chinese). Mar Geol Quat Geol, 10: 21−33
Zhou T R, Li H Z, Liu Q S, Li R Q, Sun X P. 1991. Cenozoic Paleogeography of the Nihewan Basin (in Chinese). Beijing: Science Press. 162
Zhu R, An Z, Potts R, Hoffman K A. 2003. Magnetostratigraphic dating of early humans in China. Earth-Sci Rev, 61: 341–359
Zhu R X, Deng C L, Pan Y X. 2007. Magnetochronology of the fluvio-lacustrine sequences in the Nihewan basin and its implications for early human colonization of northeast Asia (in Chinese). Quat Sci, 27: 922−944
Zhu R X, Hoffman K A, Potts R, Deng C L, Pan Y X, Guo B, Shi C D, Guo Z T, Yuan B Y, Hou Y M, Huang W W. 2001. Earliest presence of humans in northeast Asia. Nature, 413: 413–417
Zhu R, Liu Q, Pan Y, Deng C, Zhang R, Wang X. 2006. No apparent lock-in depth of the Laschamp geomagnetic excursion: Evidence from the Malan loess. Sci China Ser D-Earth Sci, 49: 960–967
Zhu R, Pan Y, Liu Q. 1999. Geomagnetic excursions recorded in Chinese Loess in the last 70,000 years. Geophys Res Lett, 26: 505–508
Zhu R X, Potts R, Pan Y X, Lü L Q, Yao H T, Deng C L, Qin H F. 2008a. Paleomagnetism of the Yuanmou Basin near the southeastern margin of the Tibetan Plateau and its constraints on late Neogene sedimentation and tectonic rotation. Earth Planet Sci Lett, 272: 97–104
Zhu R X, Potts R, Pan Y X, Yao H T, Lü L Q, Zhao X, Gao X, Chen L W, Gao F, Deng C L. 2008b. Early evidence of the genus *Homo* in East Asia. J Human Evol, 55: 1075–1085
Zhu R X, Potts R, Xie F, Hoffman K A, Deng C L, Shi C D, Pan Y X, Wang H Q, Shi R P, Wang Y C, Shi G H, Wu N Q. 2004. New evidence on the earliest human presence at high northern latitudes in northeast Asia. Nature, 431: 559–562
Zhu R, Zhang R, Deng C, Pan Y, Liu Q, Sun Y. 2007. Are Chinese loess deposits essentially continuous? Geophys Res Lett, 34: L17306
Zhu R X, Zhou L P, Laj C, Mazaud A, Ding Z L. 1994. The Blake geomagnetic polarity episode recorded in Chinese loess. Geophys Res Lett, 21: 697–700
Zhu W L, Wang Z F, Mi L J, Du X B, Xie X N, Lu Y C, Zhang D J, Sun Z P, Liu X Y, You L. 2015a. Sequence stratigraphic framework and reef growth unit of Well Xike-1 from Xisha Islands, South China Sea (in Chinese). Earth Sci—J China Univ Geosci, 40: 677−687
Zhu Z Y, Dennell R, Huang W W, Wu Y, Rao Z G, Qiu S F, Xie J B, Liu W, Fu S Q, Han J W, Zhou H Y, Ou Yang T P, Li H M. 2015b. New dating of the *Homo erectus* cranium from Lantian (Gongwangling), China. J Human Evol, 78: 144–157
Zuo T W, Cheng H J, Liu P, Xie F, Deng C L. 2012. Magnetostratigraphic dating of the Hougou Paleolithic site in the Nihewan Basin, North China. Sci China Earth Sci, 54: 1643–1650

(Responsible editor: Shuzhong SHEN)